Burning rates in hybrid rocket motors

- Burning rates – begin comparing with solid propellants; what about liquids in rocket motors – differences in mechanisms
- A general simple approach to modeling – invoking the analogy of gaseous fuels – premixed and diffusion
- Measurement techniques, early results, conflicts and resolution – PJP devoted
- The broad results on burn rate with various fuel-oxidizer combinations
- Reconciling these results with the model
- Some other aspects
- Summary

H S Mukunda
hsm.cgpl@gmail.com; course@VSSC_21st October 2019

It is normal to expect

- that the burn rate of solid rocket propellants depends largely on pressure: $\dot{r} = a\, p_c^n$ (p_c = chamber pressure) and initial temperature dependence of burn rate is small or not important for space rocket motors.
- that the regression rate of hybrid rocket fuels depends on mass flux past the surface: $\dot{r} = a\, G^n$ (G = mass flux through the port)
- Burn rate of liquids in liquid rockets is not sought for. On the other hand, what is used in liquid rockets is a quantity called $L^* = V_c/A_t$.

Why are these ideas like this?

- Solid rockets have propellants containing both oxidizer and fuel and so can burn on their own. Their burn rate depends on the reaction rate between oxidizer and fuel that depends on p_c
- Hybrid motor fuel regression rate depends on heat transfer from the diffusion flame created between the fuel vapor and oxidizer. This depends on the flow rate and is not dependent on pressure
- Liquid rockets will have liquids are injected through orifices of fine spaces (or at least one of them) so that drop atomization is the key process that controls the conversion process. This takes some length or say, characteristic length – L^* (It will depend on the chamber diameter that gets indirectly involved through the choice of L^*) for droplet combustion to be completed. What matters is drop evaporation.

Premixed flame

Diffusion flame

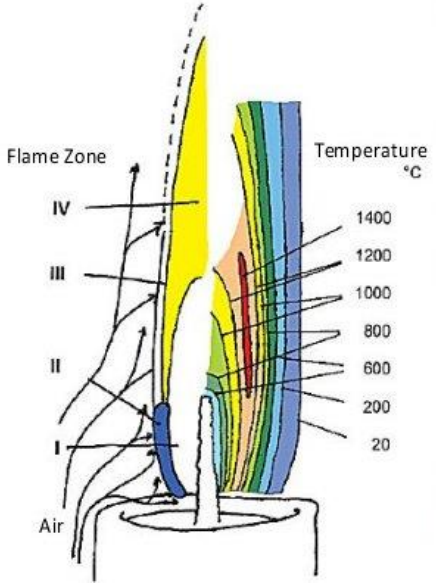

Premixed
Flame speed
~ 0.4 m/s
(Hydrocabon – air)

~ 2.5 m/s for Hydrogen - air

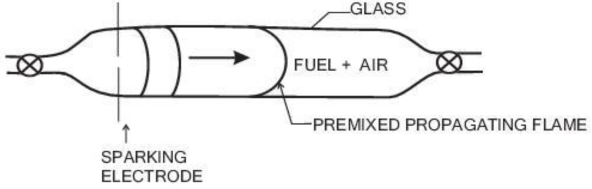

(a) Propagating Flame Apparatus

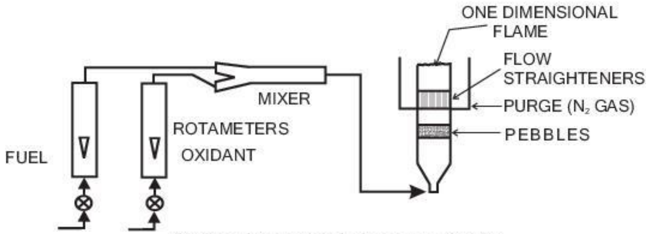

(b) One dimensional Flame Apparatus

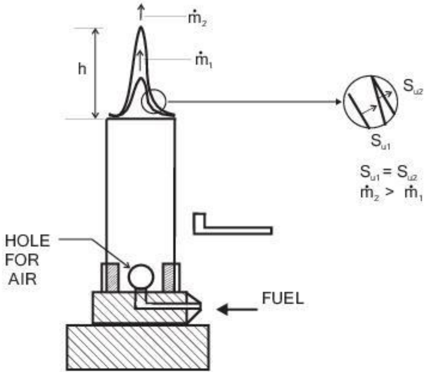

Premixed /Diffusion

From: Gross and Beckstead (2000)

Particle size effect on AP/HTPB propellant

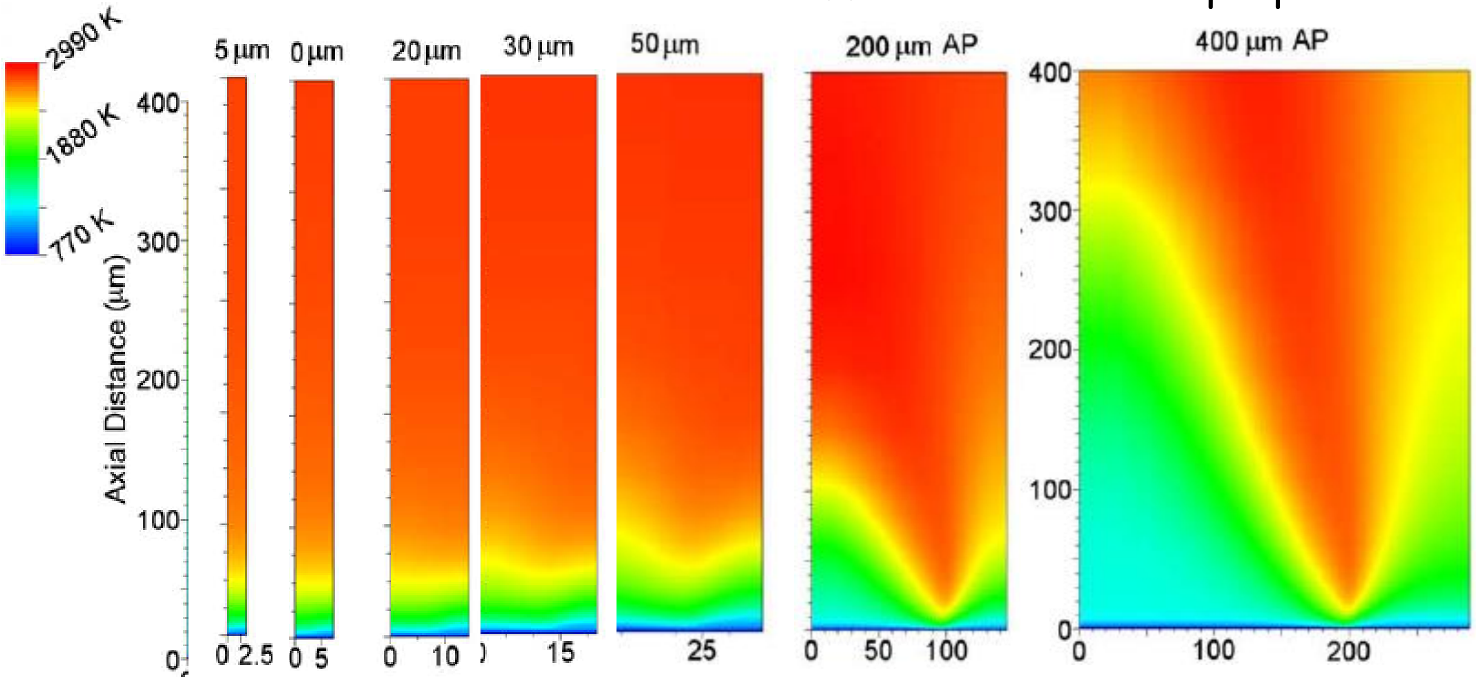

The reaction zone is smaller for premixed condition compared to Diffusion limited combustion

This is the crucial reason for lower regression rates in hybrids compared to solids

In the accompanying video, the LPG fuel – air premixed gas mean speed is
(~500 cm^3/s)/(2 cm^2)~ 2.5 m/s
six times the premixed flame speed and that is why the flame is long conical

The diffusion flame has to draw air from the ambient. This is slow and so the flame is longer

Basic physics and some thermo-chemistry

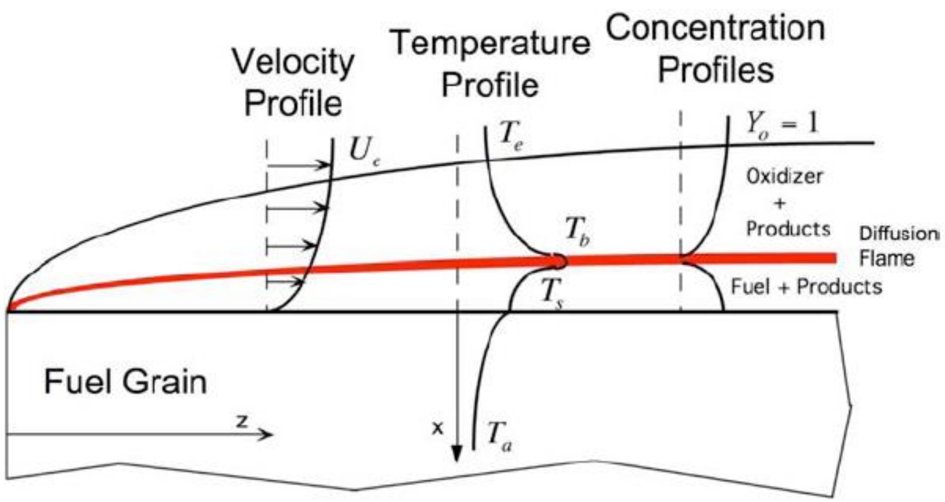

- In a “strong” diffusion flame, chemistry is very fast compared to diffusion. Hence, the flame is thin.
- Therefore, the burn rate Is controlled by diffusion rate which is affected by boundary layer next to the regressing fuel surface
- To obtain the dependence of burn rate flux on flow velocity and thermochemical parameters, we use Reynolds Analogy

The heat flux balance at the surface gives $\rho_p \dot{r} \Delta H_s = q'' = k\, dT/dy\big]_s \sim k\, dT/dU\;\; dU/dy \sim k(T_f - T_s)/U\;\; 1/\mu\;\; \mu dU/dy \sim$ $(k/c_p\mu)\, c_p(T_f - T_s)/U\, \tau_w \sim (k/c_p\mu)\, c_p(T_f - T_s)/U\;\; (cf/2)\, \rho U^2 \sim (k/c_p\mu)\, c_p(T_f - T_s)\;\; \underline{(c_f/c_{f0})}\, (c_{f0}/2)\, \rho U$

[$\rho_p \dot{r}$ = fuel/propellant mass flux from the surface; ΔH_s = *Heat of phase change*; $\underline{(c_f/c_{f0})}$ = *Blocking effect*]

From this, we get: $\rho_p \dot{r} \sim (k/c_p\mu)\, [c_p(T_f - T_s)/\, \Delta H_s]\, \underline{(c_f/c_{f0})}\, (c_{f0}/2)\, \rho U \sim (1/Pr)\, B\, \underline{[\ln(1+B)/B]}\, \rho U\, [0.054\, (\rho U)^{-0.2}] \sim C_0 \ln(1+B)\, G^{0.8}$
where **$B = [c_p(T_f - T_s)/\, \Delta H_s]$; $G = \rho U$; $\ln(1+B)$ is sometimes treated as $B^{0.25}$ in the range of B’s relevant**

Thus $\rho_p \dot{r} = C_0\, B^{0.25}\, G^{0.8}$

This indicates that that thermochemical parameters characterized by B have little influence on $\rho_p \dot{r}$

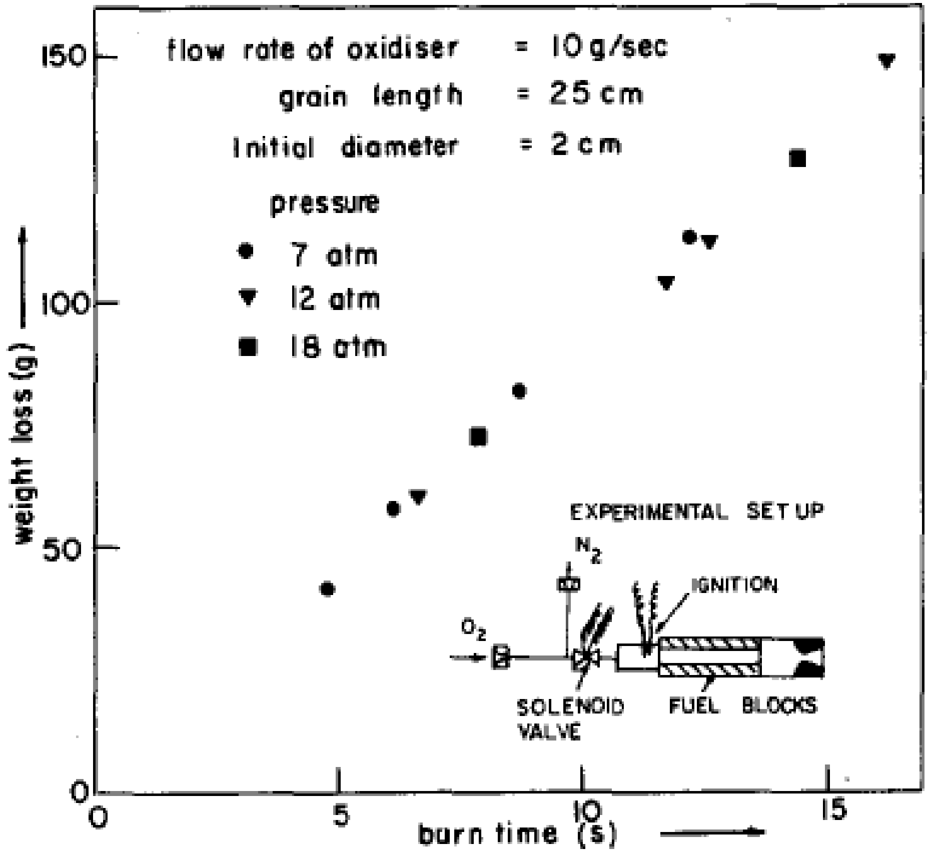

FIG. 2. Weight loss vs. burn time at various pressures from present measurements.

The data shows that in a practical range, pressure does not influence the regression rate. This is a direct evidence for diffusion- limitedness of the phenomenon.

An examination of earlier literature reveals that no experiments have specifically been carried out to elucidate the dependence of regression rate on B. Most researchers have used different polymeric fuels and it is indeed difficult to estimate changes in B from fuel to fuel as the factor h_v in B = $\Delta h_g / h_v$ is composed of relatively less certain heat of degradation to a fragment size larger than the basic monomer. Therefore it was thought worth while conducting experiments to estimate the effect of varying B on regression rate by varying $(\Delta h)_g$. This is done by varying the gaseous composition (of say an oxygen + nitrogen mixture).

Index on B is much higher than by M & W model.
Also, reg. rate is much Higher than the results of M & W

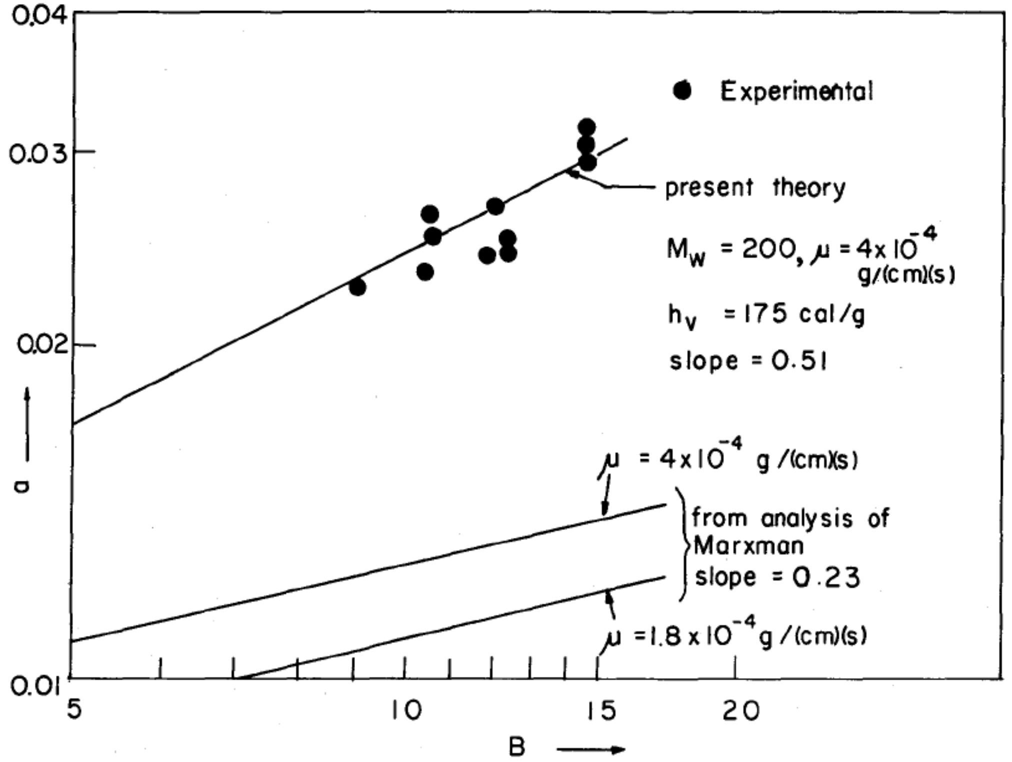

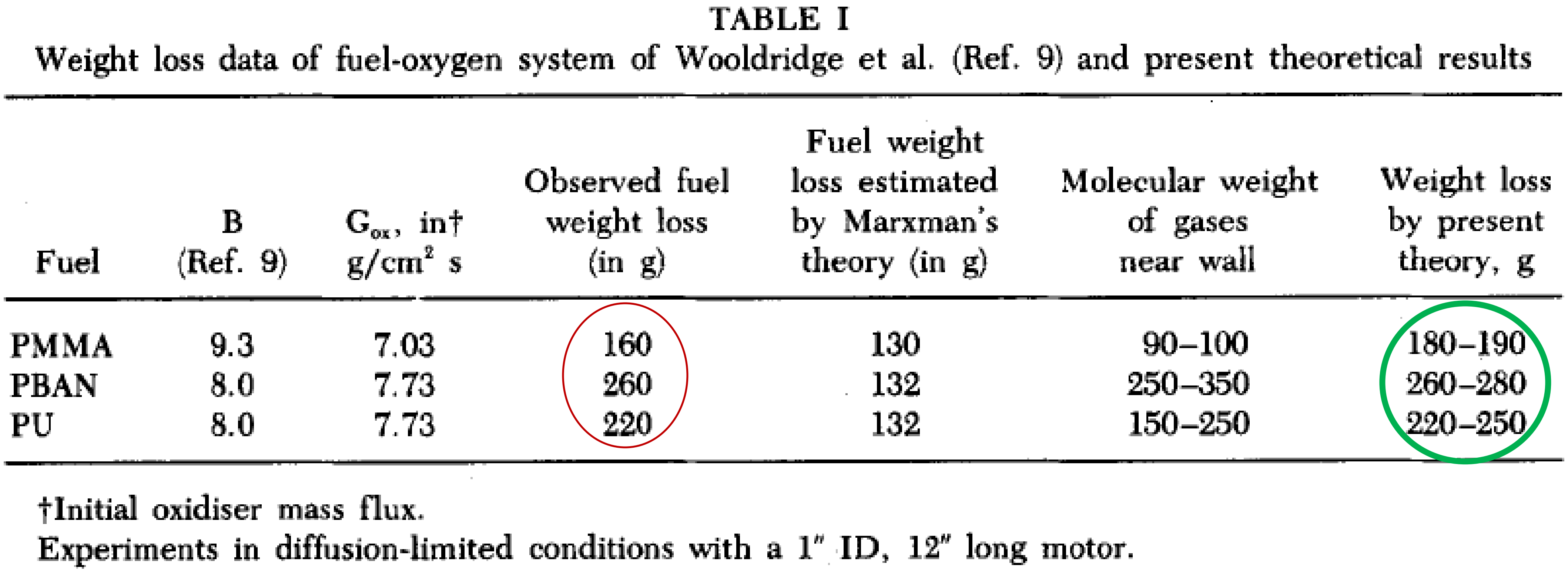

TABLE I

Weight loss data of fuel-oxygen system of Wooldridge et al. (Ref. 9) and present theoretical results

Fuel	B (Ref. 9)	G_{ox}, in† g/cm^2 s	Observed fuel weight loss (in g)	Fuel weight loss estimated by Marxman's theory (in g)	Molecular weight of gases near wall	Weight loss by present theory, g
PMMA	9.3	7.03	160	130	90–100	180–190
PBAN	8.0	7.73	260	132	250–350	260–280
PU	8.0	7.73	220	132	150–250	220–250

†Initial oxidiser mass flux.

Experiments in diffusion-limited conditions with a 1" ID, 12" long motor.

What was shown in Paul et al (1982) is that

(a) If B & W model is correct, then $\rho_p \dot{r} \sim B^{0.23}$ and therefore differences in fuel cannot have any impact on the fuel burn flux.
(b) Experimental data of M & W do not support their own model.
(c) Analyzed as due to improper accounting of blocking effect – the effect of variation of fuel injection on the boundary layer.
(d) The molecular weight of the fuel fragments coming off the fuel surface can be up to 400, the value depends on the nature of the fuel itself. This raises the density of the gas at the surface and so the density profile in the bl.
(e) This affects the estimation of blocking effect known earlier with experimental results of injection of CO2 and Freon into air
(f) This results in an expression for $\rho_p \dot{r} \sim B^{0.51}$ Modified result for the regression rate when tested against known data works better

The result of Paul et al (1982) is:

$$\rho_p \dot{r} = 0.056\, G^{0.8} \left(\frac{x}{\mu}\right)^{-0.2} (\rho_f/\rho_e)^{0.71} (\rho_w/\rho_e)^{0.14}$$

$$\cdot\, B\,(1 + B)^{-(0.73-0.002\,\rho_w/\rho_e)}$$

Other researchers have performed experiments and developed models for burn rate

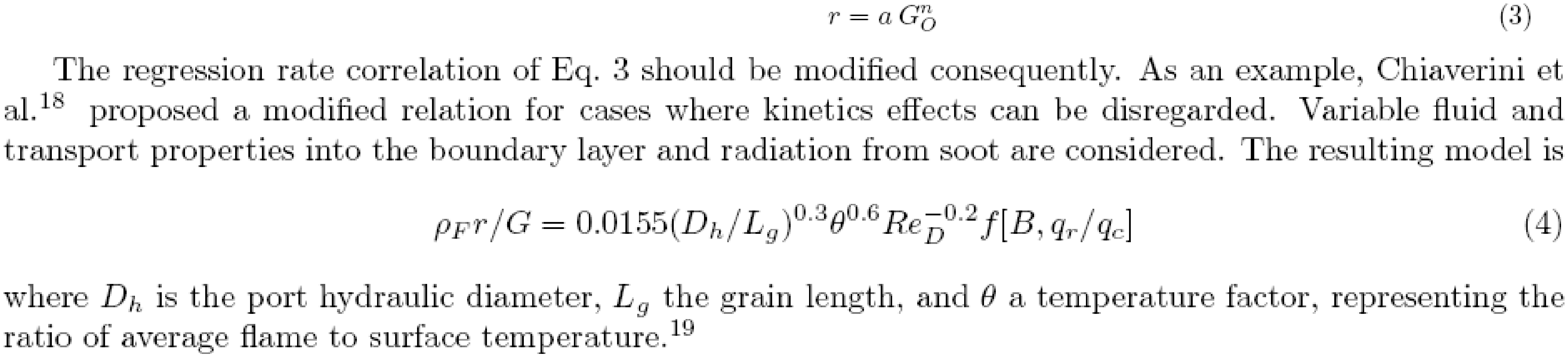

$$r = a\, G_O^n \tag{3}$$

The regression rate correlation of Eq. 3 should be modified consequently. As an example, Chiaverini et al.[18] proposed a modified relation for cases where kinetics effects can be disregarded. Variable fluid and transport properties into the boundary layer and radiation from soot are considered. The resulting model is

$$\rho_F r/G = 0.0155(D_h/L_g)^{0.3}\theta^{0.6} Re_D^{-0.2} f[B, q_r/q_c] \tag{4}$$

where D_h is the port hydraulic diameter, L_g the grain length, and θ a temperature factor, representing the ratio of average flame to surface temperature.[19]

There is considerable similarity in the final expressions recommended to be adopted recently and the earlier result derived by P. J. Paul. Yet, the expression that is adopted is given by eqn (3).

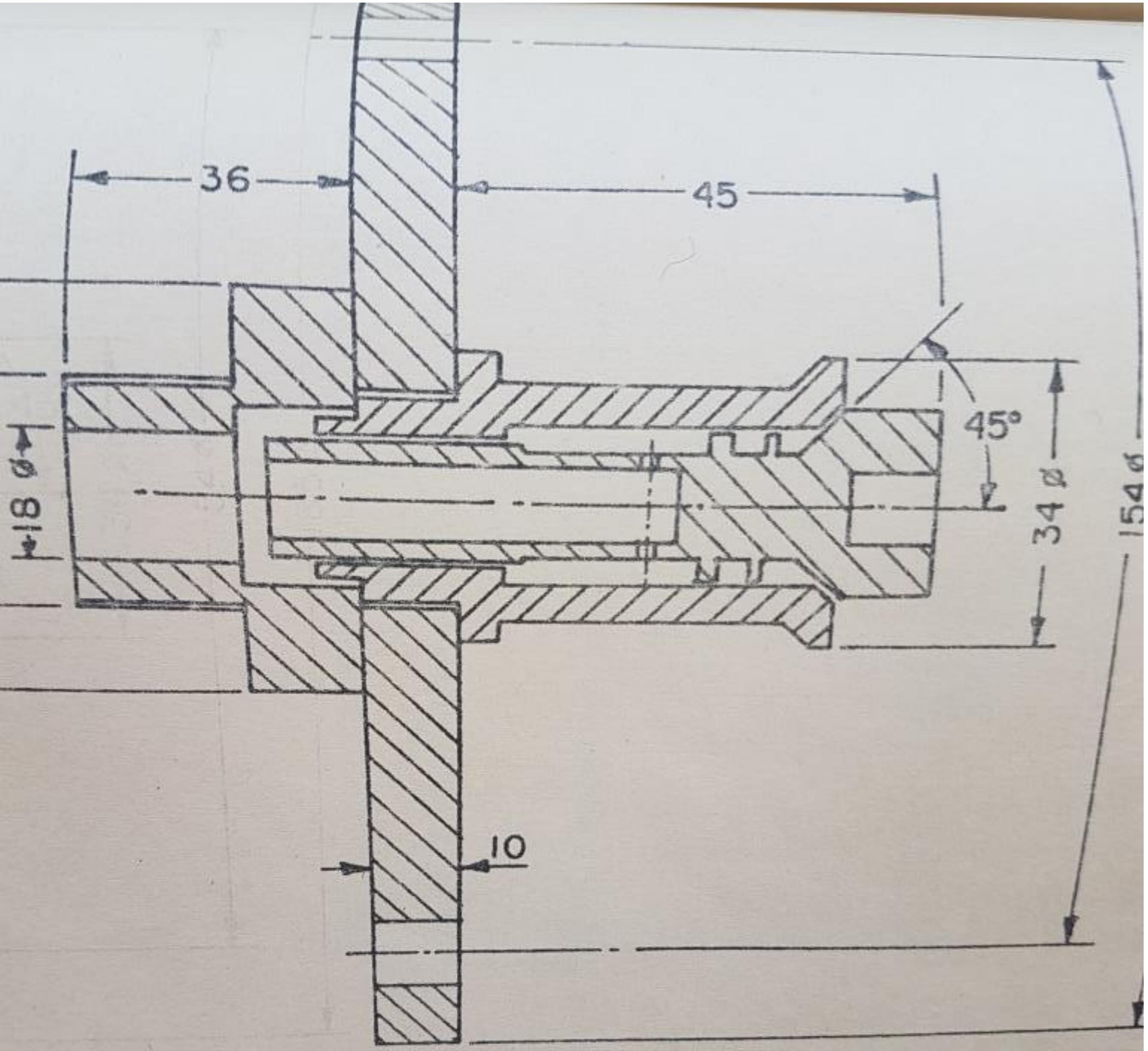

(c)

FIG. 4.3 SECTIONAL VIEW OF THE INJECTOR

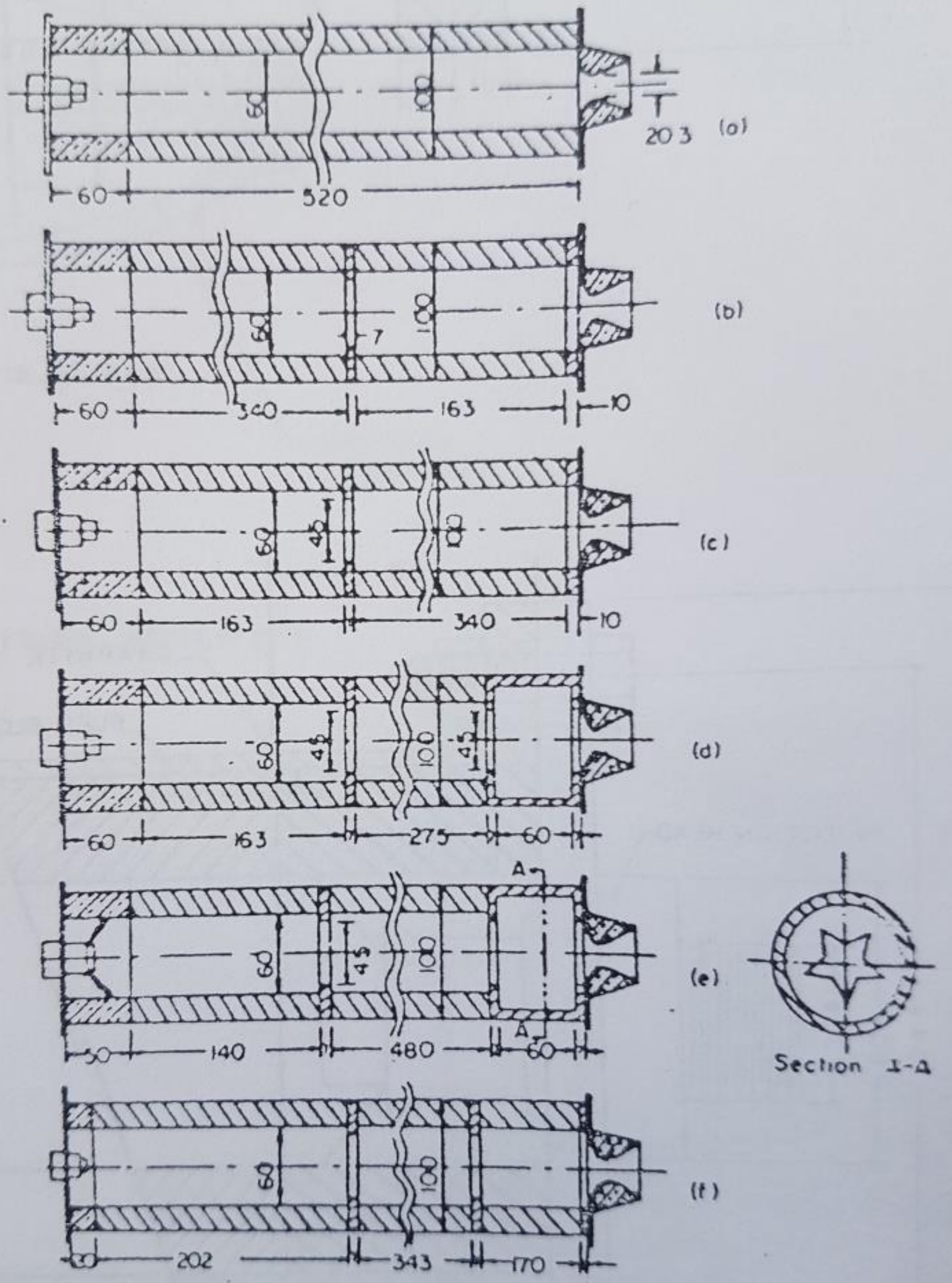

FIG 13 CONFIGURATIONS FOR THE FIRINGS OF SUSTAINER

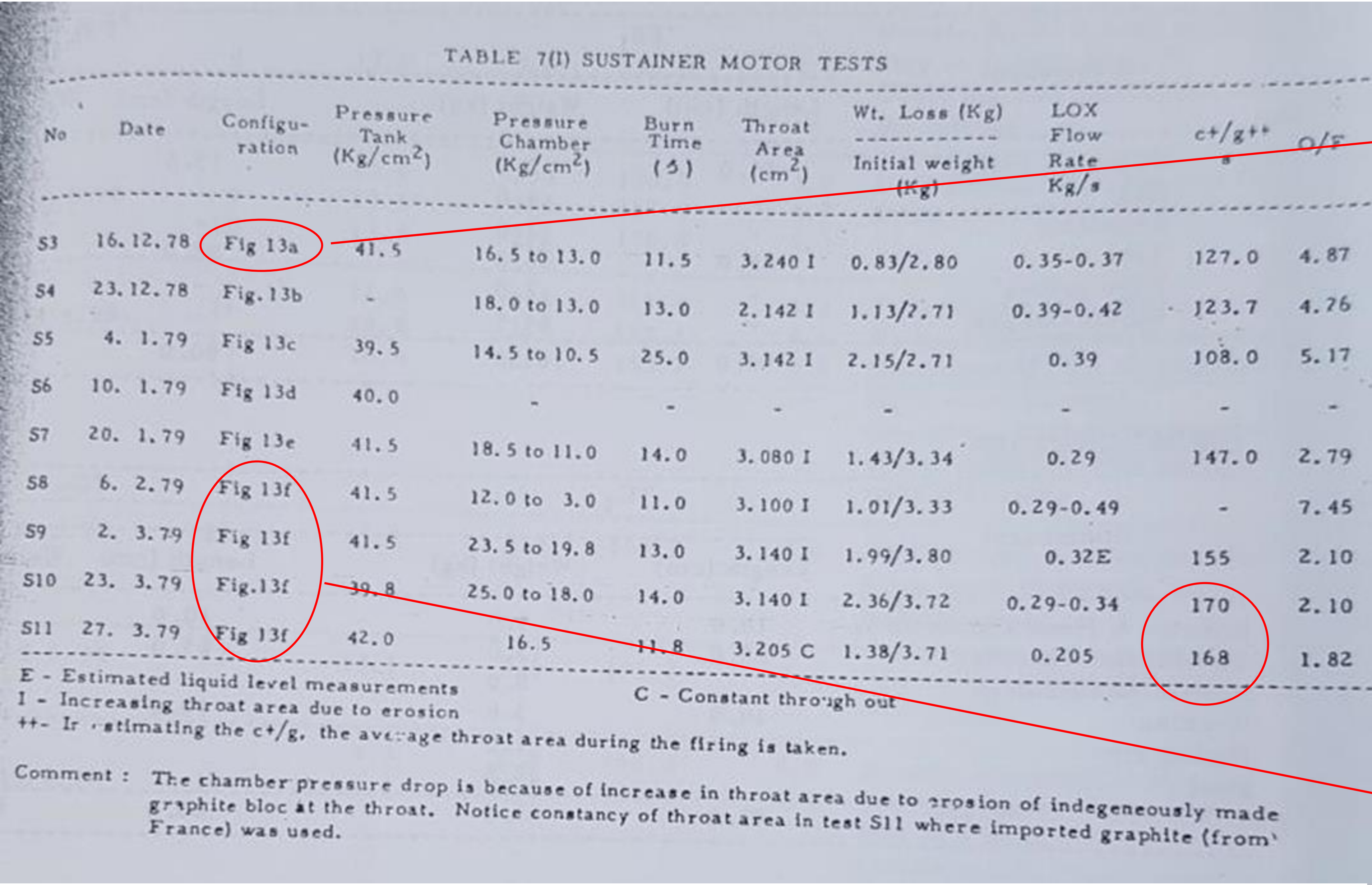

TABLE 7(I) SUSTAINER MOTOR TESTS

No	Date	Configuration	Pressure Tank (Kg/cm^2)	Pressure Chamber (Kg/cm^2)	Burn Time (s)	Throat Area (cm^2)	Wt. Loss (Kg) / Initial weight (Kg)	LOX Flow Rate Kg/s	c+/g++	O/F
S3	16. 12. 78	Fig 13a	41. 5	16. 5 to 13. 0	11. 5	3. 240 I	0. 83/2. 80	0. 35-0. 37	127. 0	4. 87
S4	23. 12. 78	Fig. 13b	-	18. 0 to 13. 0	13. 0	2. 142 I	1. 13/2. 71	0. 39-0. 42	123. 7	4. 76
S5	4. 1. 79	Fig 13c	39. 5	14. 5 to 10. 5	25. 0	3. 142 I	2. 15/2. 71	0. 39	108. 0	5. 17
S6	10. 1. 79	Fig 13d	40. 0	-	-	-	-	-	-	-
S7	20. 1. 79	Fig 13e	41. 5	18. 5 to 11. 0	14. 0	3. 080 I	1. 43/3. 34	0. 29	147. 0	2. 79
S8	6. 2. 79	Fig 13f	41. 5	12. 0 to 3. 0	11. 0	3. 100 I	1. 01/3. 33	0. 29-0. 49	-	7. 45
S9	2. 3. 79	Fig 13f	41. 5	23. 5 to 19. 8	13. 0	3. 140 I	1. 99/3. 80	0. 32E	155	2. 10
S10	23. 3. 79	Fig. 13f	39. 8	25. 0 to 18. 0	14. 0	3. 140 I	2. 36/3. 72	0. 29-0. 34	170	2. 10
S11	27. 3. 79	Fig 13f	42. 0	16. 5	11. 8	3. 205 C	1. 38/3. 71	0. 205	168	1. 82

E - Estimated liquid level measurements

I - Increasing throat area due to erosion

C - Constant through out

++- In estimating the c+/g, the average throat area during the firing is taken.

Comment : The chamber pressure drop is because of increase in throat area due to erosion of indegeneously made graphite bloc at the throat. Notice constancy of throat area in test S11 where imported graphite (from France) was used.

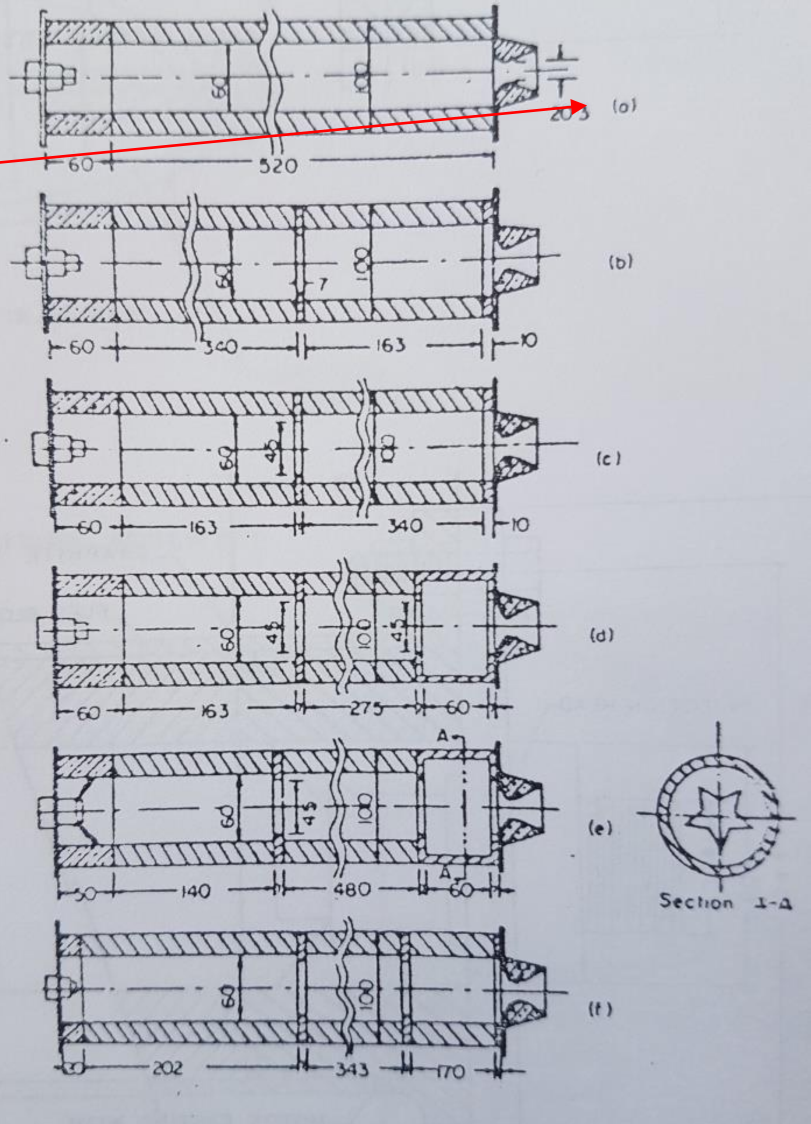

FIG 13 CONFIGURATIONS FOR THE FIRINGS OF SUSTAINER

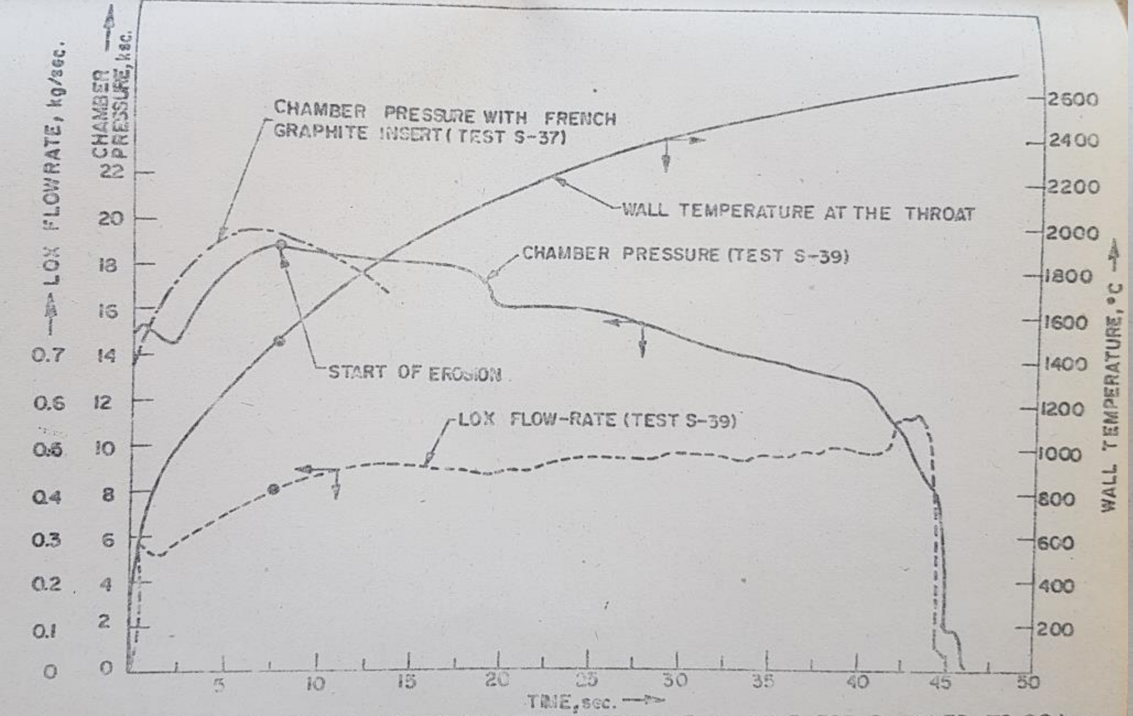

13 PRESSURE, FLOW-RATE (LOX), AND SURFACE TEMPERATURE Vs. TIME FOR P_c TUNED TO 20 ksc. WITH PYROLYTIC GRAPHITE INSERT (NOZZLE OF FIG.5.11) AND INSULATION BETWEEN GRAPHIT AND STEEL. WALL TEMPERATURE AT THE THROAT IS COMPUTED FOR P_c = 20 ksc., T_c = 3231°K, C^* = 1563 m/sec., $\dot{m}_{ox}$ = 0.42 kg/sec., O/F = 2.8

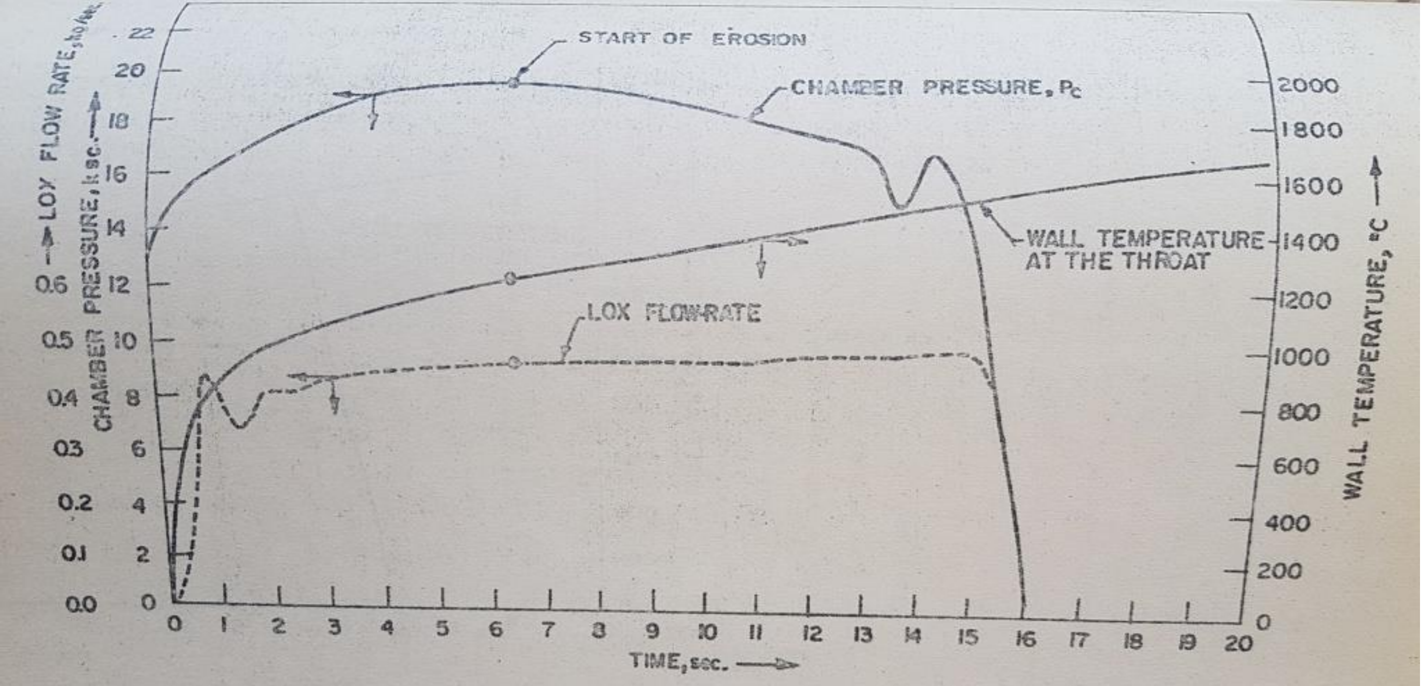

FIG.5.7 PRESSURE, FLOWRATE (LOX), AND SURFACE TEMPERATURE Vs. TIME FOR P_c TUNED TO 20 ksc. WITH FRENCH GRAPHITE INSERT (NOZZLE OF FIG.5.6). WALL TEMPERATURE AT THE THROAT IS COMPUTED FOR P_c = 20 ksc., T_c = 3231°K., C^* = 1563 m/sec., $\dot{m}_{ox}$ = 0.42 kg/sec., O/F = 2.8

IISc data:
GOX-(Natural rubber + Synaprene)
$\dot{r} = 3.1 \times 10^{-5} G_{ox}^{0.5}$ m/s, Gox = kg/m^{2}s

Problems & Pitfalls

- The burn rates in literature are often obtained from mass loss
  - Problems with this approach
    - Nonlinear behavior of the burn rate over time generates a wrong average
    - Non-uniform regression

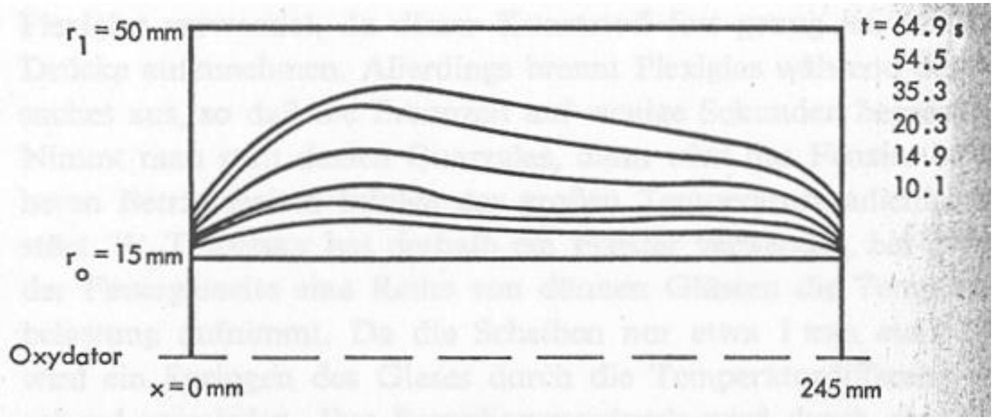

example of non-uniform regression

- One must be careful when interpreting results for experiments with oxygen. The differences between LOX and GOX are large, but which one was used is not always very well documented (e.g. Sutton Fig. 15-6).

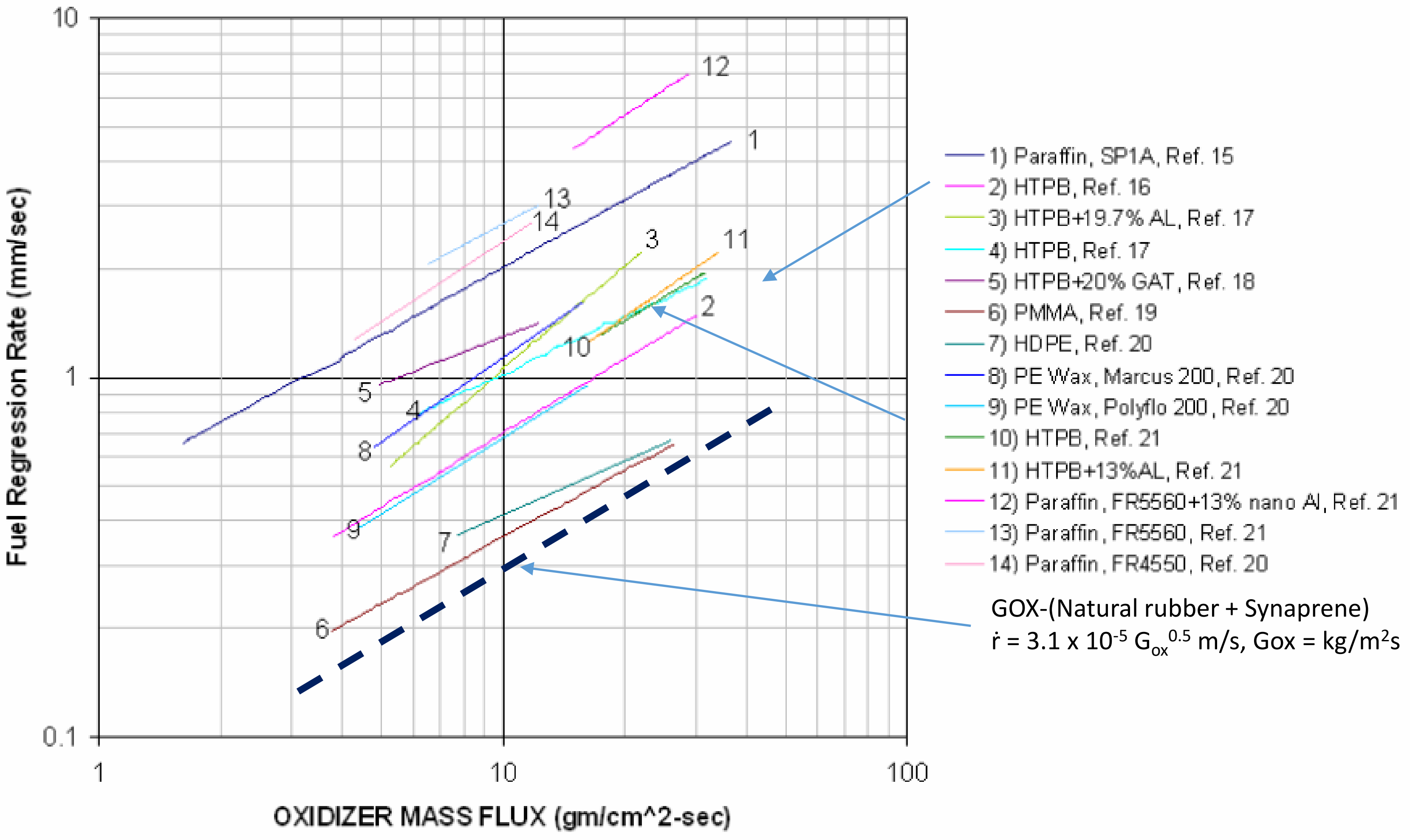

GOX-(Natural rubber + Synaprene)
$\dot{r} = 3.1 \times 10^{-5} G_{ox}^{0.5}$ m/s, Gox = kg/m^{2}s

Zilliac, G. G., and Karebayaglu,
Hybrid regression rate data
and modeling, AIIA 2006-4054,
42nd AIAA-ASME
Joint Prop. conf.

….Many factors including scale, O/F, combustion configuration, injector design, fuel composition (trace additives included) and processing, data reduction and experimental techniques impact the accuracy of the data presented……the actual regression rate of a fuel and oxidizer Combination should be independently verified.

My comments: (a) I agree with the general observations. (b) The data scatter is such that all the above data may actually be described by $\dot{r} = a\, G_{ox}^{n}$ with n = 0.5 within the error bounds of the experiments (c) The most accurate Information is weight loss over a certain time and should be determined to ensure the data is reproducible. All analysis done at IISc were performed in this manner.

Regression rate vs mass flux on various fuels by researchers

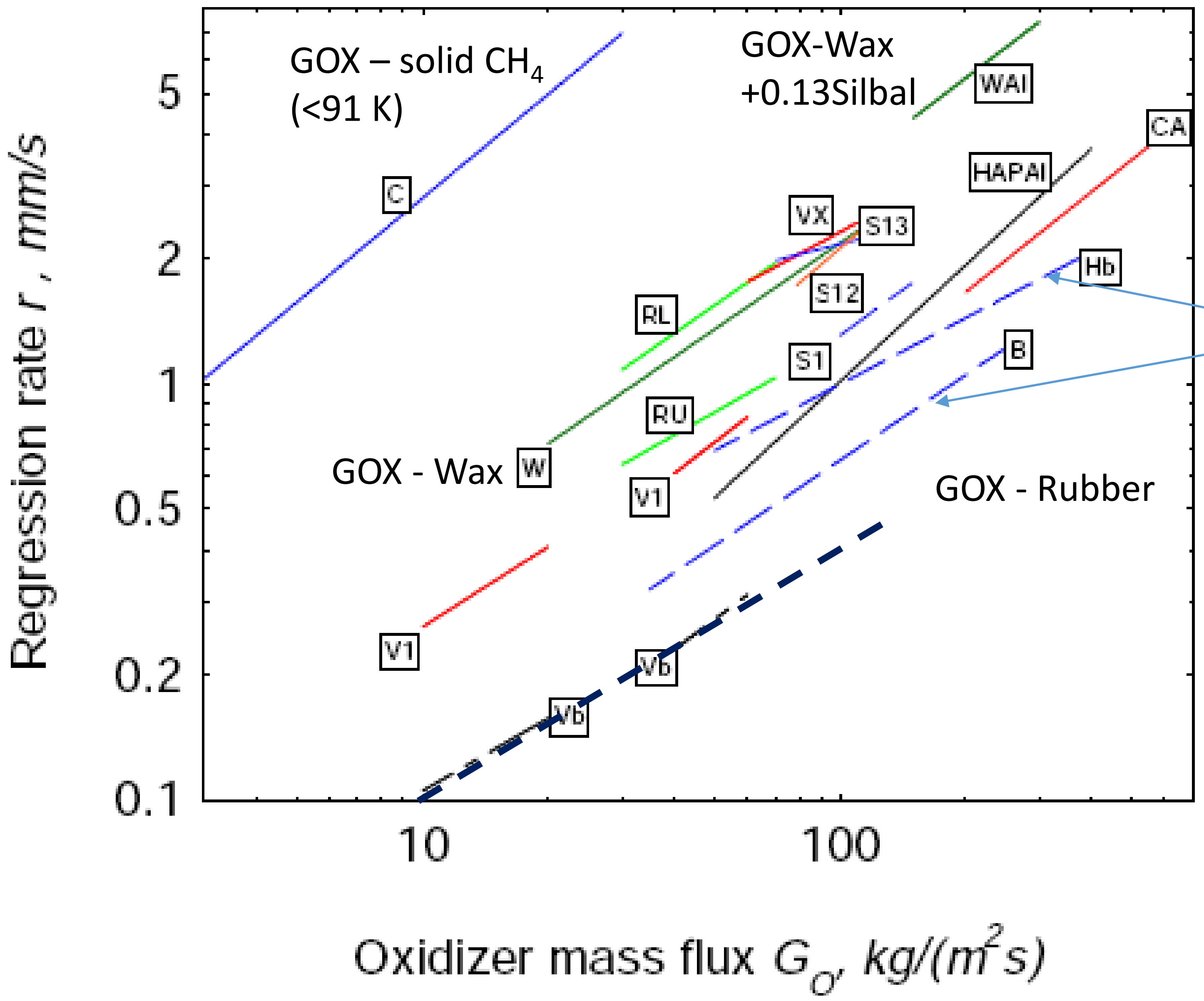

B and Hb: LOX-HTPB
by two different studies

GOX-(Natural rubber + Synaprene)
$\dot{r} = 0.031\, G_{ox}^{0.5}$ mm/s, G_{ox} = kg/m^{2}s

D. G. Pastrone, Approaches to low fuel regression rate in hybrid rocket engines, Int. J. Aerospace Engg, 2012

Data on regression rates (Pastrone, 2012)

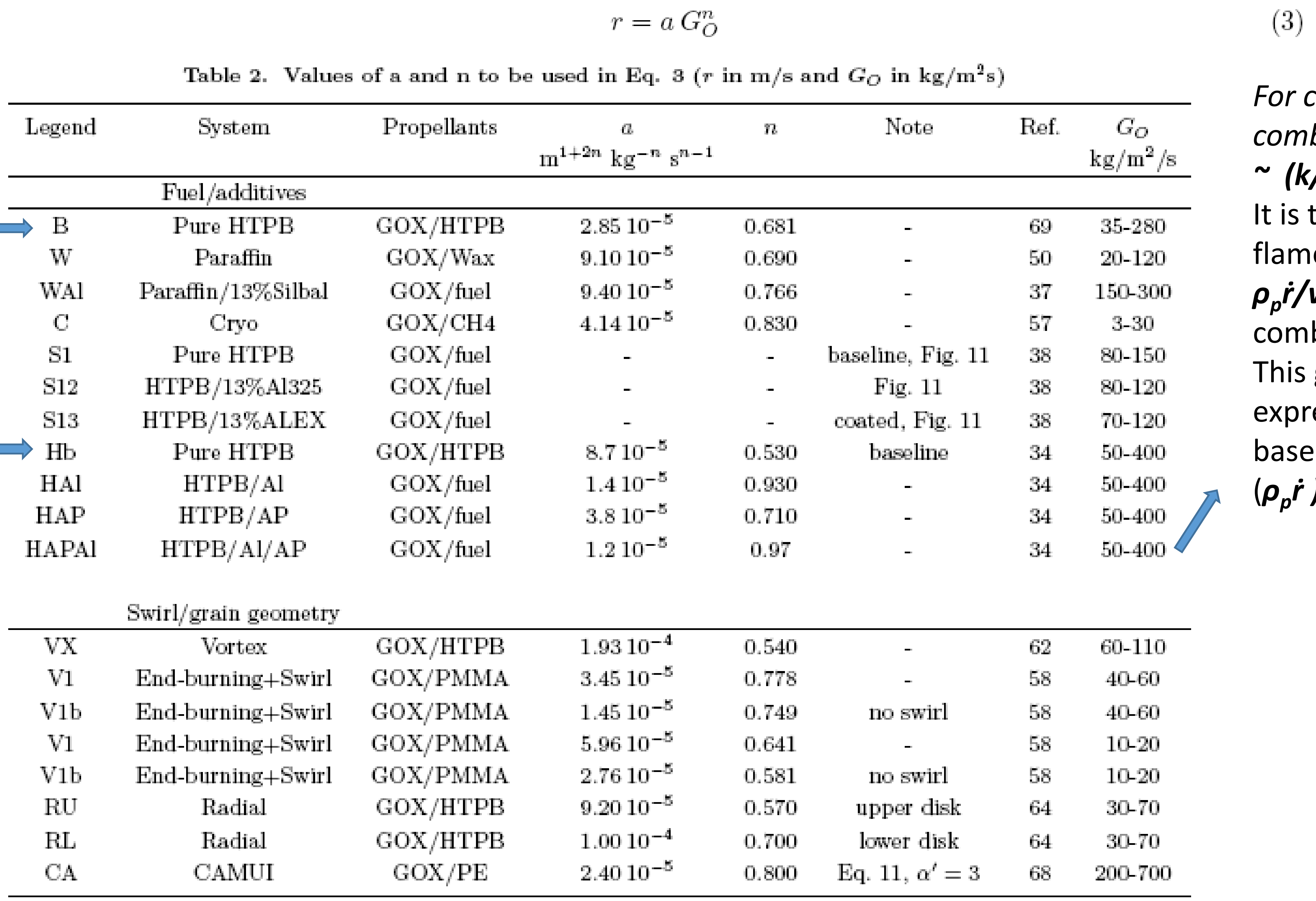

$$r = a\,G_O^n \qquad (3)$$

Table 2. Values of a and n to be used in Eq. 3 (r in m/s and G_O in kg/m^{2}s)

Legend	System	Propellants	a m^{1+2n} kg^{-n} s^{n-1}	n	Note	Ref.	G_O kg/m^2/s
	Fuel/additives						
B	Pure HTPB	GOX/HTPB	$2.85\,10^{-5}$	0.681	-	69	35-280
W	Paraffin	GOX/Wax	$9.10\,10^{-5}$	0.690	-	50	20-120
WAl	Paraffin/13%Silbal	GOX/fuel	$9.40\,10^{-5}$	0.766	-	37	150-300
C	Cryo	GOX/CH4	$4.14\,10^{-5}$	0.830	-	57	3-30
S1	Pure HTPB	GOX/fuel	-	-	baseline, Fig. 11	38	80-150
S12	HTPB/13%Al325	GOX/fuel	-	-	Fig. 11	38	80-120
S13	HTPB/13%ALEX	GOX/fuel	-	-	coated, Fig. 11	38	70-120
Hb	Pure HTPB	GOX/HTPB	$8.7\,10^{-5}$	0.530	baseline	34	50-400
HAl	HTPB/Al	GOX/fuel	$1.4\,10^{-5}$	0.930	-	34	50-400
HAP	HTPB/AP	GOX/fuel	$3.8\,10^{-5}$	0.710	-	34	50-400
HAPAl	HTPB/Al/AP	GOX/fuel	$1.2\,10^{-5}$	0.97	-	34	50-400
	Swirl/grain geometry						
VX	Vortex	GOX/HTPB	$1.93\,10^{-4}$	0.540	-	62	60-110
V1	End-burning+Swirl	GOX/PMMA	$3.45\,10^{-5}$	0.778	-	58	40-60
V1b	End-burning+Swirl	GOX/PMMA	$1.45\,10^{-5}$	0.749	no swirl	58	40-60
V1	End-burning+Swirl	GOX/PMMA	$5.96\,10^{-5}$	0.641	-	58	10-20
V1b	End-burning+Swirl	GOX/PMMA	$2.76\,10^{-5}$	0.581	no swirl	58	10-20
RU	Radial	GOX/HTPB	$9.20\,10^{-5}$	0.570	upper disk	64	30-70
RL	Radial	GOX/HTPB	$1.00\,10^{-4}$	0.700	lower disk	64	30-70
CA	CAMUI	GOX/PE	$2.40\,10^{-5}$	0.800	Eq. 11, $\alpha' = 3$	68	200-700

For chemistry controlled combustion, we can write $\rho_p \dot{r} \sim (k/c_p)\ B\ 1/\delta_{bl}$

It is the chemistry driven flame thickness δ_{bl} ***or*** $x^* \sim \rho_p \dot{r}/w'''$ for premixed combustion,

This gives the burn rate expression for fine particle based solid propellant :

$(\rho_p \dot{r})^2 \sim (k/c_p)\ B\ w'''$

Results summary of the average regression rate with oxygen for various fuels

No.	Fuel	$a^{\dagger}$	n	No. of Tests	Chamber Pressure Range (MPa)	Average O/F Ratio Range	Data Reduction Technique	Oxidizer Mass Flux Range (g/cm^2-sec)	Ref.
1	Paraffin, SP1A	0.488	0.62	65	1.1-6.9	1.0-4.0	DA	1.6-36.9	15
2	HTPB, (Thiokol)	0.146	0.681	16	-	-	-	3.8-30.2	16
3	HTPB+19.7%AL	0.117	0.956	2	1.2	-	OA	5.1-23.0	17
4	HTPB	0.304	0.527	3	2.0	-	OA	6.2-31.0	17
5	HTPB+20%GAT	0.473	0.439	5	-	-	-	-	18
6	PMMA	0.087	0.615	8	0.3-2.6	-	-	3.3-26.6	19
7	HDPE	0.132	0.498	4	0.7-1.3	3.8-5.9	DA	7.7-26.1	20
8	PE Wax, Marcus 200	0.188	0.781	4	0.5-1.2	2.2-3.2	DA	4.8-15.8	20
9	PE Wax, Polyflo 200	0.134	0.703	3	0.6-1.2	1.6-1.7	DA	4.4-16.3	20
10	HTPB	0.194	0.670	6	-	-	OA	17.5-32.0	21
11	HTPB+13% nano Al	0.145	0.775	12	-	-	OA	16.5-34.2	21
12	Paraffin, FR5560 + 13% nano Al	0.602	0.730	8	-	-	OA	14.5-29.0	21
13	Paraffin, FR5560	0.672	0.600	4	-	-	OA	6.3-12.3	21
14	Paraffin, FR4550	0.427	0.748	3	0.7-?	1.3-1.8	DA	4.3-11.9	20

Regression rate equation: $\bar{\dot{r}} = a\overline{G}_o{}^{n} x^{m}$ with $m = 0$

[†] For use with G_o with units of gm/cm^2-sec, produces an average regression rate in mm/sec.

DA: Diameter Averaged, FA: Flux Averaged, AA: Area Average, OA: Other averaging technique applied

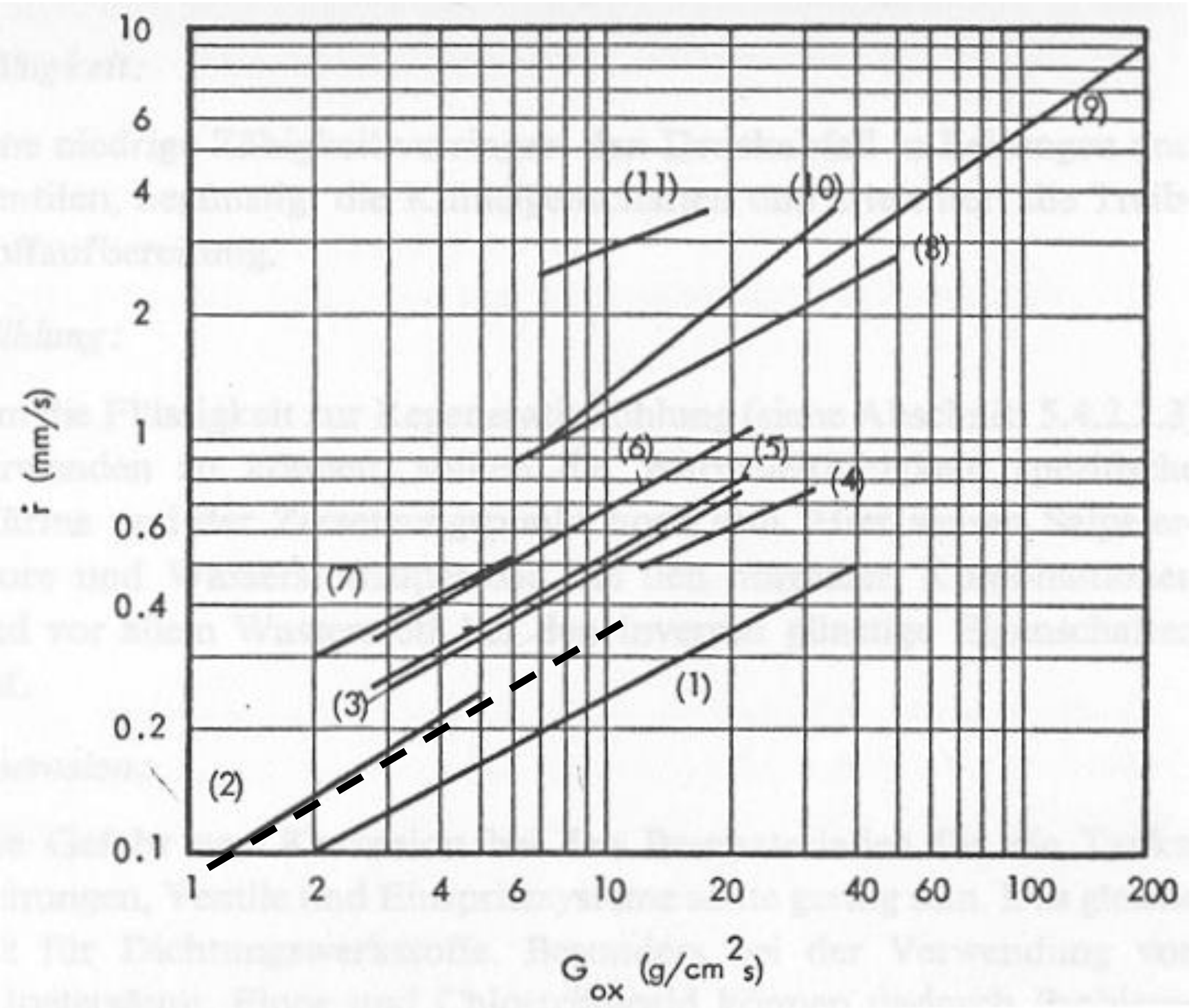

1. PMMA - Oxygen
2. PMMA - Oxygen
3. PMMA - Oxygen
4. PE - H_2O_2
5. Rubber - N_2O_4
6. Rubber (metalized) - N_2O_4
7. PE - FLOX
8. p-Toluidin/p-Aminophenol -HNO_3 - Swedish work
9. p-Toluidin/PVC-HNO_3 - Swedish work
10. Tagaform-HNO_3 - Swedish work
11. $LiAlH_3$ - H_2O_2
12. Rubber - GOX-Rubber - IISc

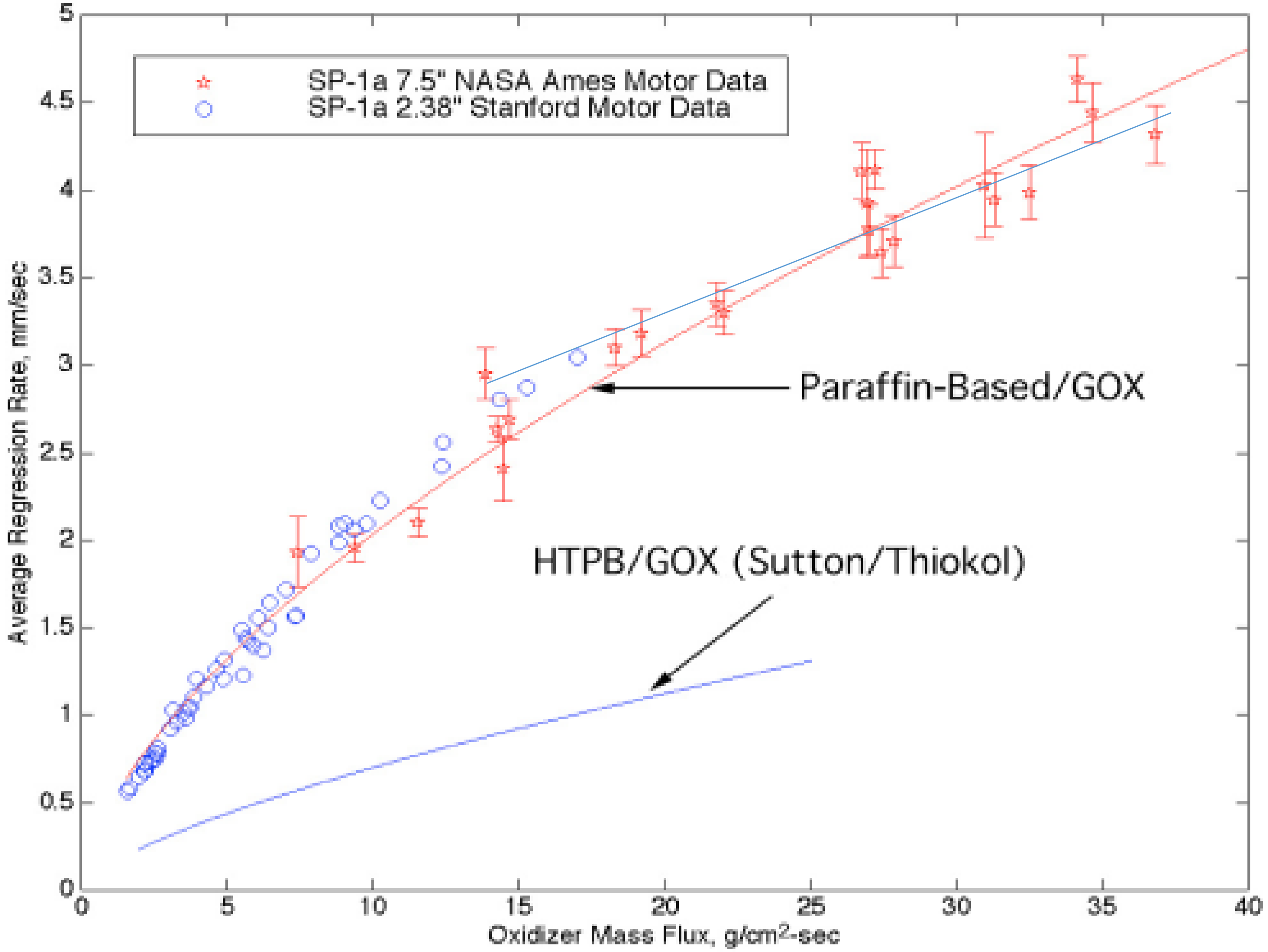

$\dot{r} = 3.2 \text{ mm/s } (G_{ox}/20)^{0.5}$

Gox in g/scm^2

Figure 11.14: *Regression rate versus oxidizer mass flux for paraffin and HTPB.*

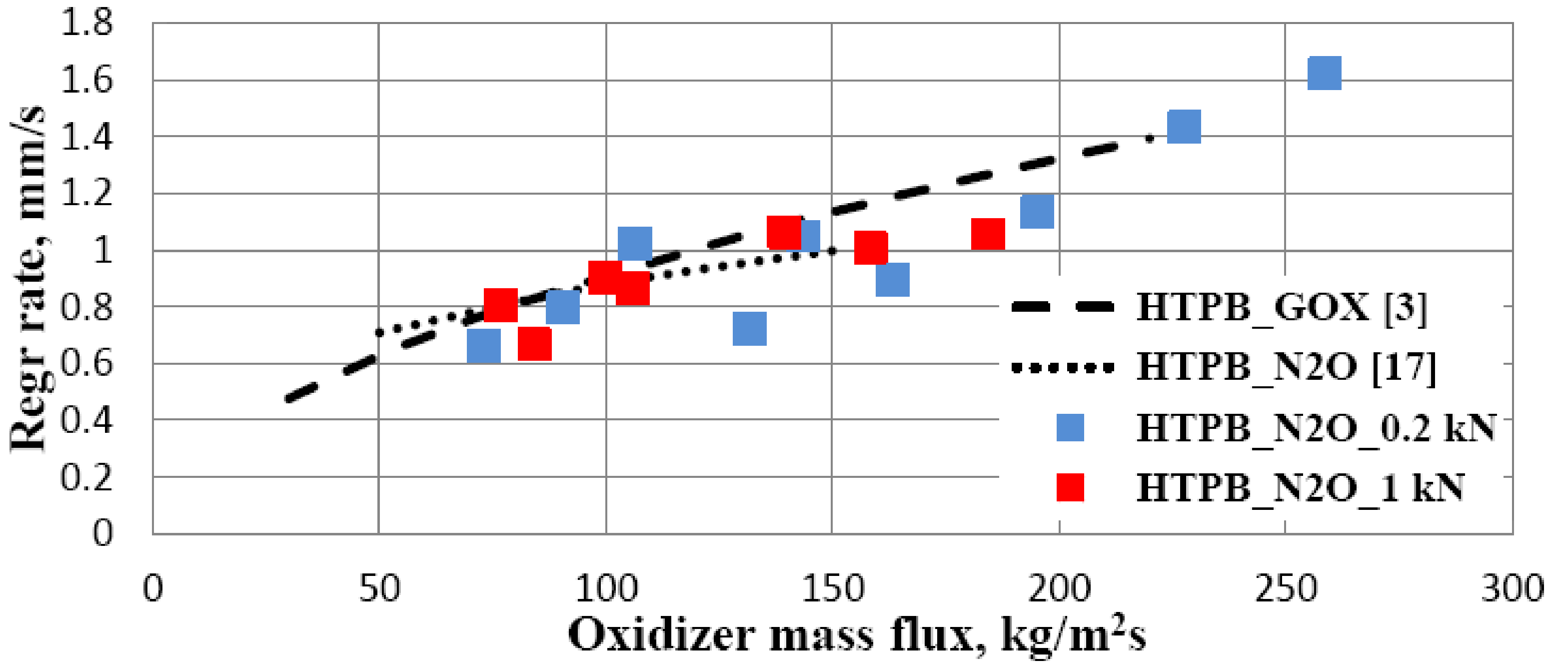

Figure 8. Average regression rate as a function of the oxidizer mass flux.

Scaramuzzoni et al, 2013

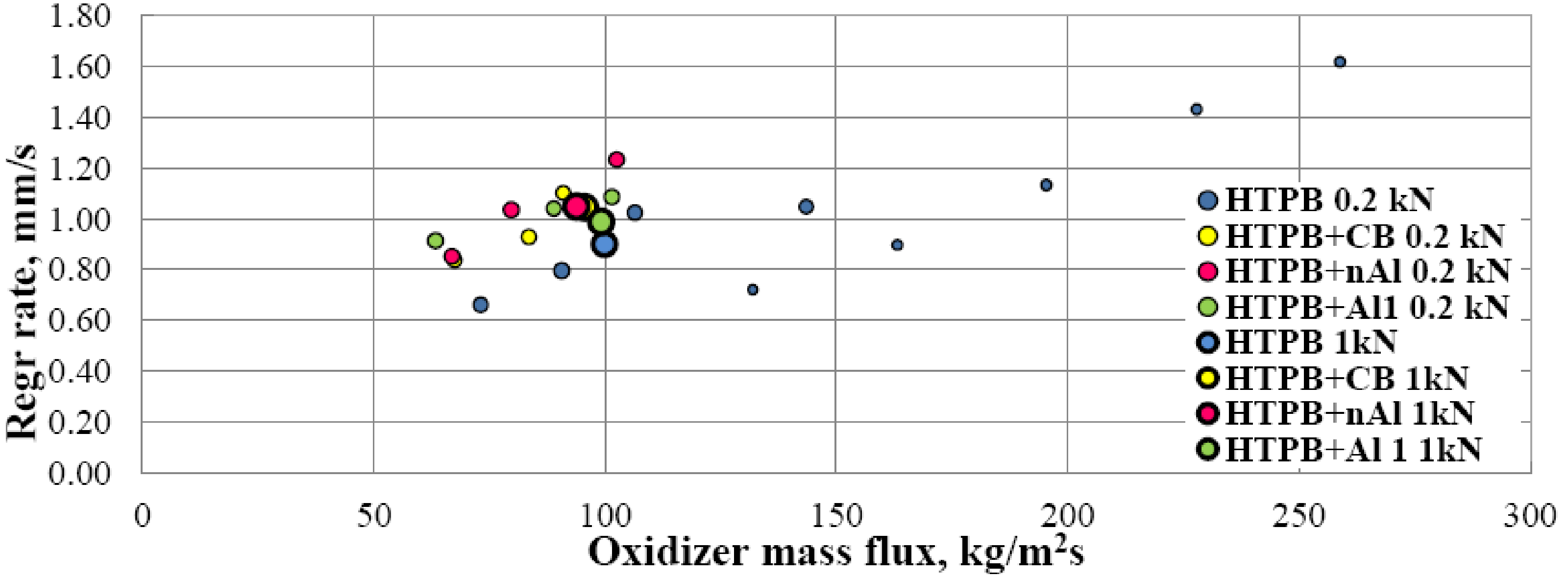

Figure 10. Average regression rate as a function of the nitrous oxide mass flux; bubble size is proportional to average port diameters.

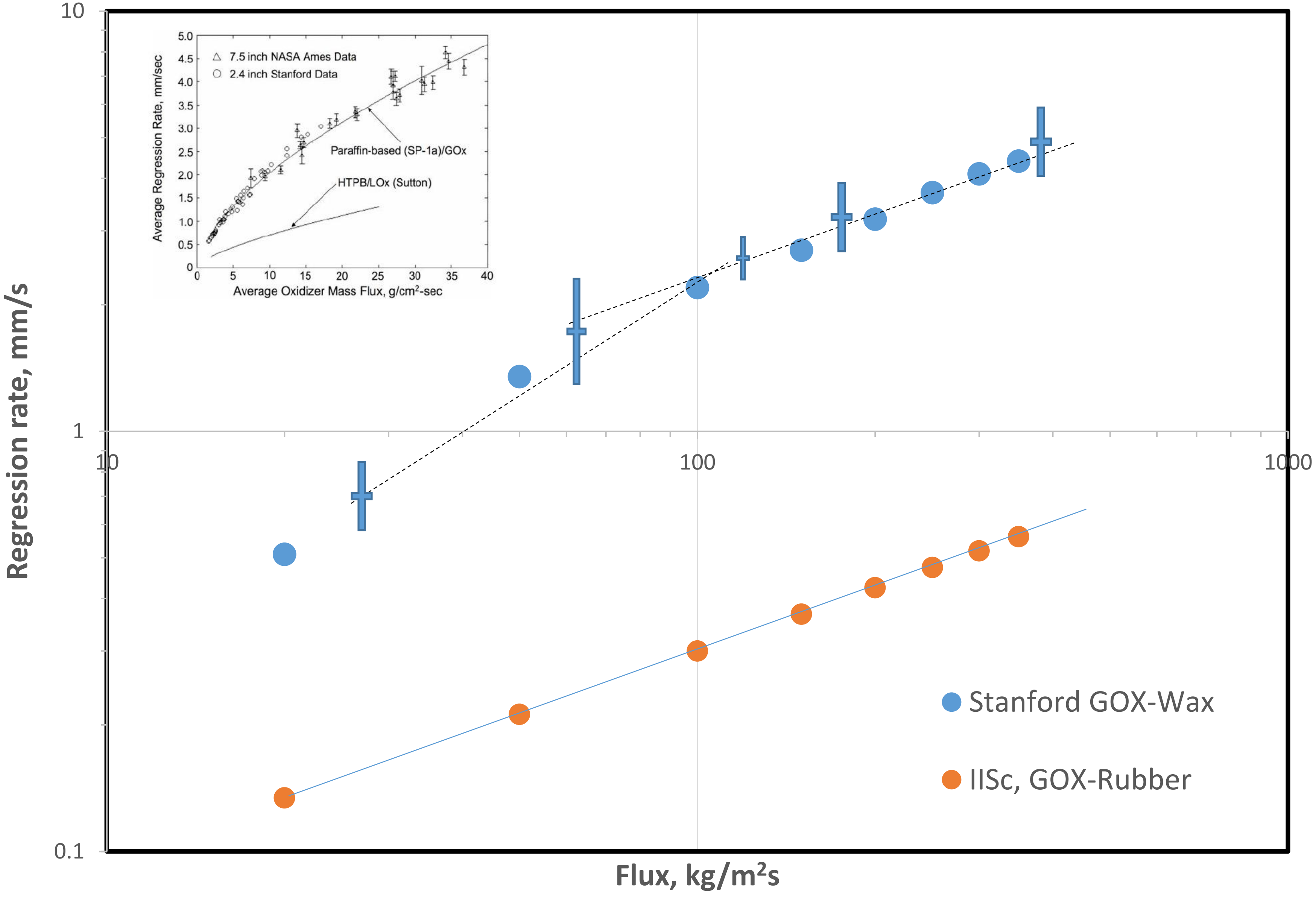

10
1
0.1
10
100
1000
Regression rate, mm/s
Flux, kg/m²s
Stanford GOX-Wax
IISc, GOX-Rubber
5.0
4.5
4.0
3.5
3.0
2.5
2.0
1.5
1.0
0.5
0
0
5
10
15
20
25
30
35
40
7.5 inch NASA Ames Data
2.4 inch Stanford Data
Paraffin-based (SP-1a)/GOx
HTPB/LOx (Sutton)
Average Regression Rate, mm/sec
Average Oxidizer Mass Flux, g/cm²-sec

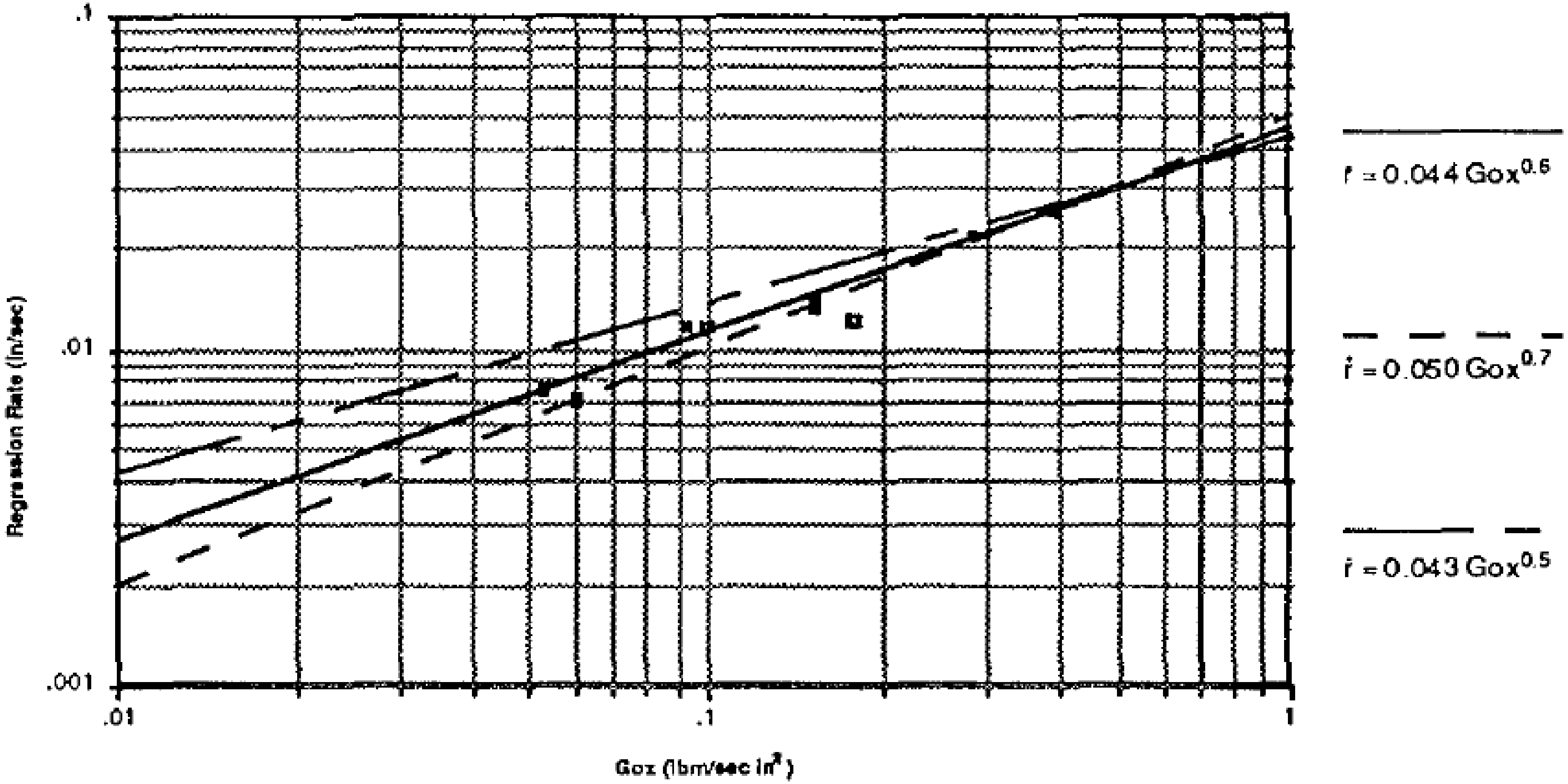

Figure 6. PMMA Regression Rate Results.

Question: The authors have set out the above plot. If we take it that they are correct, does it matter a whole lot which burn rate law we choose as long as they are within the data band?

My answer: It does not.

Swirl Injection Effects on Hybrid Rocket Motors

Susane Ribeiro Gomes[1], Leopoldo Rocco[2], José Atílio Fritz F. Rocco[3]

HDPE fuel with the use of axial and swirl injectors.

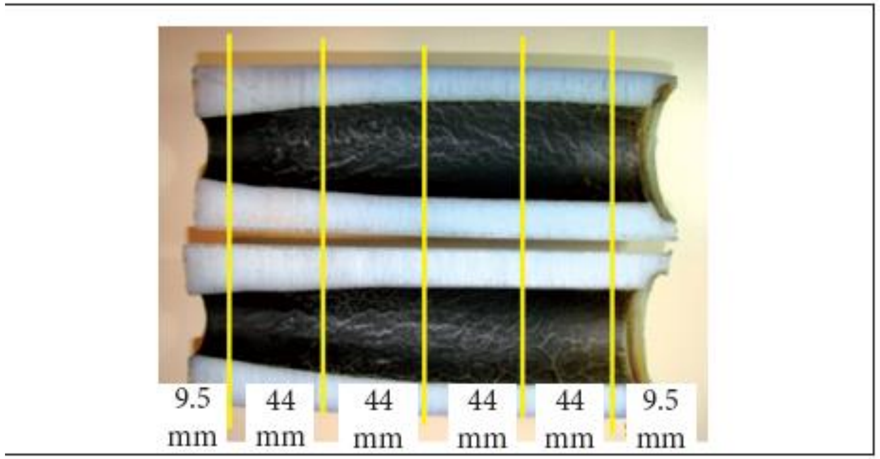

gure 6. Cross-sections for the calculation of mean gression rate.

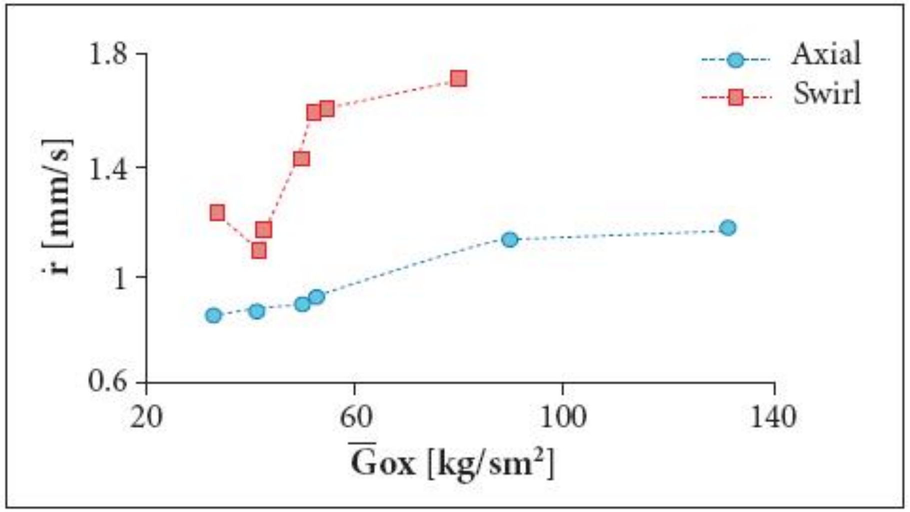

Figure 6. Regression rate *versus* oxidizer mass flux for each injection method.

Table 4. Constant *n* found experimentally for the regression rate equation.

Reference	Injector	Oxidizer/fuel	*n*
Myre *et al.* (2010)	Swirl	$\overline{G}_{ox}$/PE	0.5
Carmicino and Russo Sorge (2005a)	Swirl	$\overline{G}_{ox}$/PE	0.5
Carmicino and Russo Sorge (2005b)	Axial	$\overline{G}_{ox}$/PE	0.371
Carmicino and Russo Sorge (2005b)	Swirl	$\overline{G}_{ox}$/PE	0.5
Knuth *et al.* (2002)	Swirl	$\overline{G}_{ox}$/HTPB	0.54
Yuasa *et al.* (2001)	Swirl	$\overline{G}_{ox}$/PMMA	0.641
Nagata *et al.* (2011)	Swirl	CAMUI	0.8
Present research	Swirl	$\overline{G}_{ox}$/PE	**0.52**
Present research	Axial	$\overline{G}_{ox}$/PE	0.26

Solid-Fuel Regression Rate Modeling for Hybrid Rockets

F. M. Favaró[*] and W. A. Sirignano[†]
University of California, Irvine, Irvine, California 92697

JOURNAL OF PROPULSION AND POWER
Vol. 29, No. 1, January–February 2013

M. Manzoni[‡] and L. T. DeLuca[§]
Politecnico di Milano, 20156 Milan, Italy

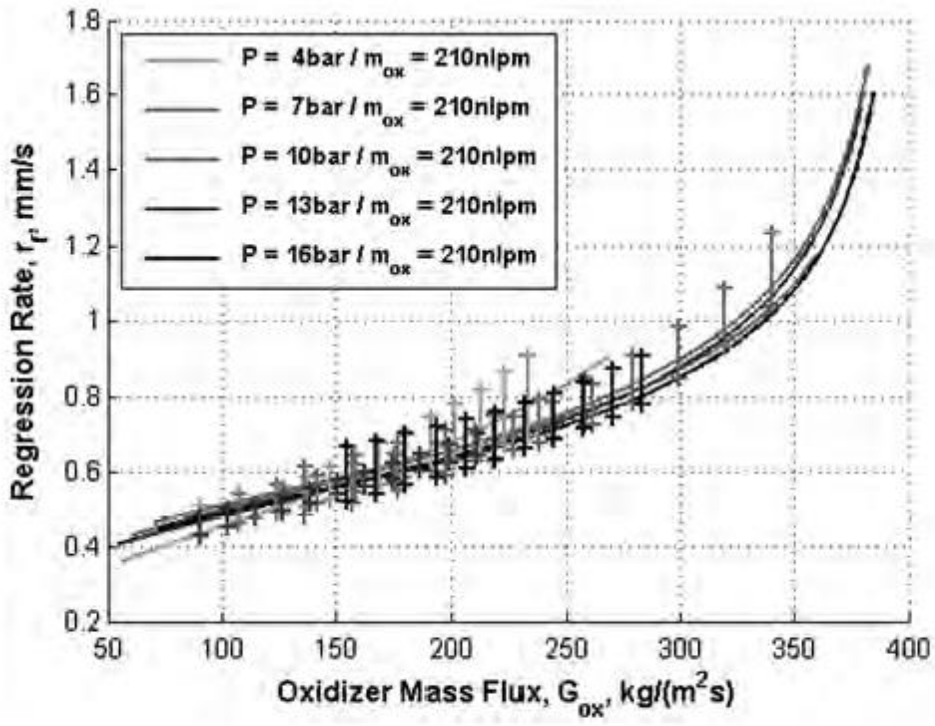

Fig. 5 Instantaneous ensemble regression rate showing negligible pressure dependence within the explored operating conditions.

$$\dot{r} - \left[A(c + (\rho_s Y_{o_s})^n)\exp\left(-\frac{E_1}{T_s}\right) - B\exp\left(-\frac{E_2}{T_s}\right) - C(\rho_s Y_{f_s})\right] = 0 \tag{61}$$

where $\dot{r}$ is now a column vector containing all of the experimental results for the different values of G_{ox} and p, with $\rho_s Y_{o_s}$, T_s, and $\rho_s Y_{f_s}$ also column vectors, it is possible to get the values for the fitting constants:

$$A = 9.811e-3, \qquad c = 1.562e-2,$$

$$n = 2.781e-4 \quad B = 3.048e-2, \qquad C = 6.314e-7$$

Table 2 Example of pressure sensitivity of the different variables after corrections for $G_{\mathrm{ox}} = 250\ \mathrm{kg/(m^2 s)}$

p, bar	$\dot{r}$, mm/s	T_s, K	T_{fl}, k	Y_{f_s}	Y_{o_s}
7	0.748	983.8	2448.1	0.7739	3.83e − 3
10	0.759	984.3	2448.1	0.7744	1.61e − 5
13	0.740	1000.3	2488.3	0.7662	4.31e − 5
16	0.726	1014.1	2488.7	0.7592	3.91e − 5

How do we decide the burn rate law with so many options?

1 $\rho_f \dot{r} = .036 \left(\frac{\bar{\rho}}{\rho_e} \right)^{0.6} \left(\frac{X}{\mu_e} \right)^{-0.2} G^{0.8} B^{0.23}$ Marxman

2 $\rho_p \dot{r} = 0.056\, G^{0.8} (x/\mu)^{-0.2} (\rho_f/\rho_e)^{0.71} (\rho_w/\rho_e)^{0.14} \cdot B\,(1 + B)^{-0.73+0.002\rho_w/\rho_e}$ IISc

3 $\rho_F r/G = 0.0155(D_h/L_g)^{0.3}\theta^{0.6} Re_D^{-0.2} f[B, q_r/q_c]$ Pastrone

4 $\dot{\hat{r}} \approx \frac{A}{\rho_f}\left[1 + 2.5C_1\left(\frac{\hat{G}_{ox}\hat{D}}{\mu_m}\right)^{-0.22}\frac{\hat{D}}{L} + 4A(k+1)\left(\hat{G}_{ox}\hat{D}\right)^{k}\frac{L}{\hat{D}}\right]\hat{G}_{ox}{}^{k+1}\hat{D}^{k}$

$$A = \frac{0.022}{\mu_m{}^{k}(T_s/T_m)^{l}}\mathrm{Pr}^{-0.6}\left(\frac{\Delta h}{h_g}\right)^{0.23}\phi_c{}^{0.77}$$

Zilliac & Karebeyoglu

$$n = k + 1$$

$$k = -0.005\left(\frac{E_a}{R_u T_s}\right) - 0.08$$

5 $r = a\, G_O^m$ IISc- from experiments

If we choose $\dot{r} = a_n\, G_{ox}^{\,n}$, how do we get n and a

$dm_{fu}/dt = \rho_p\, A_b\, \dot{r}$; This can be written as

$\rho_p\, L\, d/dt\, \{\pi(D^2 - D_0^{\,2})/4\} = \rho_p\, \pi\, D\, L\, a_n\, [\dot{m}_{ox}/(\pi\, D^2/4)]^n$; We simplify this to get

$(1/2)\, dD/dt = 2\, a_n\, [4\, \dot{m}_{ox}/\pi]^n\ \ D^{-2n}$ Which can be integrated to give

$D\,(t) = [D_0^{\,(1+2n)} + 2\, a_n\, (1+2n)\, [4\, \dot{m}_{ox}/\pi]^n\ \ t]^{[1/(1+2n)]}$ and

$m_{fu}\,(t) = \rho_p\, L\, \pi/4 \Big\{ [D_0^{\,(1+2n)} + 2\, a_n\, (1+2n)\, [4\, \dot{m}_{ox}/\pi]^n\ \ t]^{[2/(1+2n)]}\ \ - D_0^{\,2} \Big\}$

$= 2\, \pi^{0.5}\, \rho_p\, L\, a_n\ \ \dot{m}_{ox}^{\,0.5}\ \ t$ for $n = 0.5$ It is linear in t

If we have m_{fu} at specific burn times then we get a_n for specific choice of n; We examine two cases with $n = 0.5$ *and* $n = 0.7$ as found in correlations. You can change these parameters in an excel sheet and see what happens.

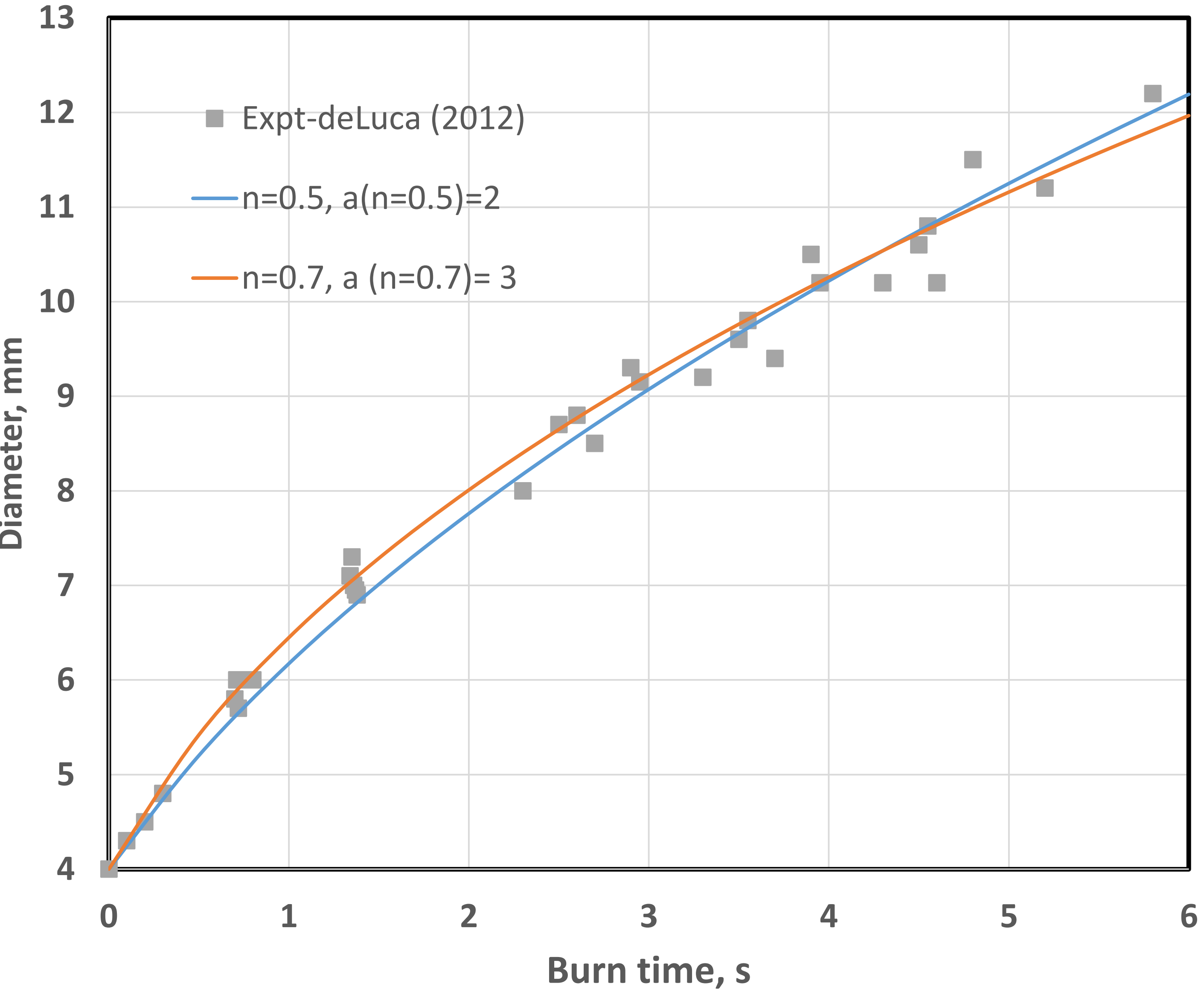

- The experimental data which is nearly always in a limited range is not particularly sensitive to the choice of n.

- For larger fluxes, n = 0.5 is a truly more appropriate choice because at larger fluxes, the role of radiation flux will be slightly larger and this reduces the index.

What about non-circular grains?
Star, Wagon wheel, etc?

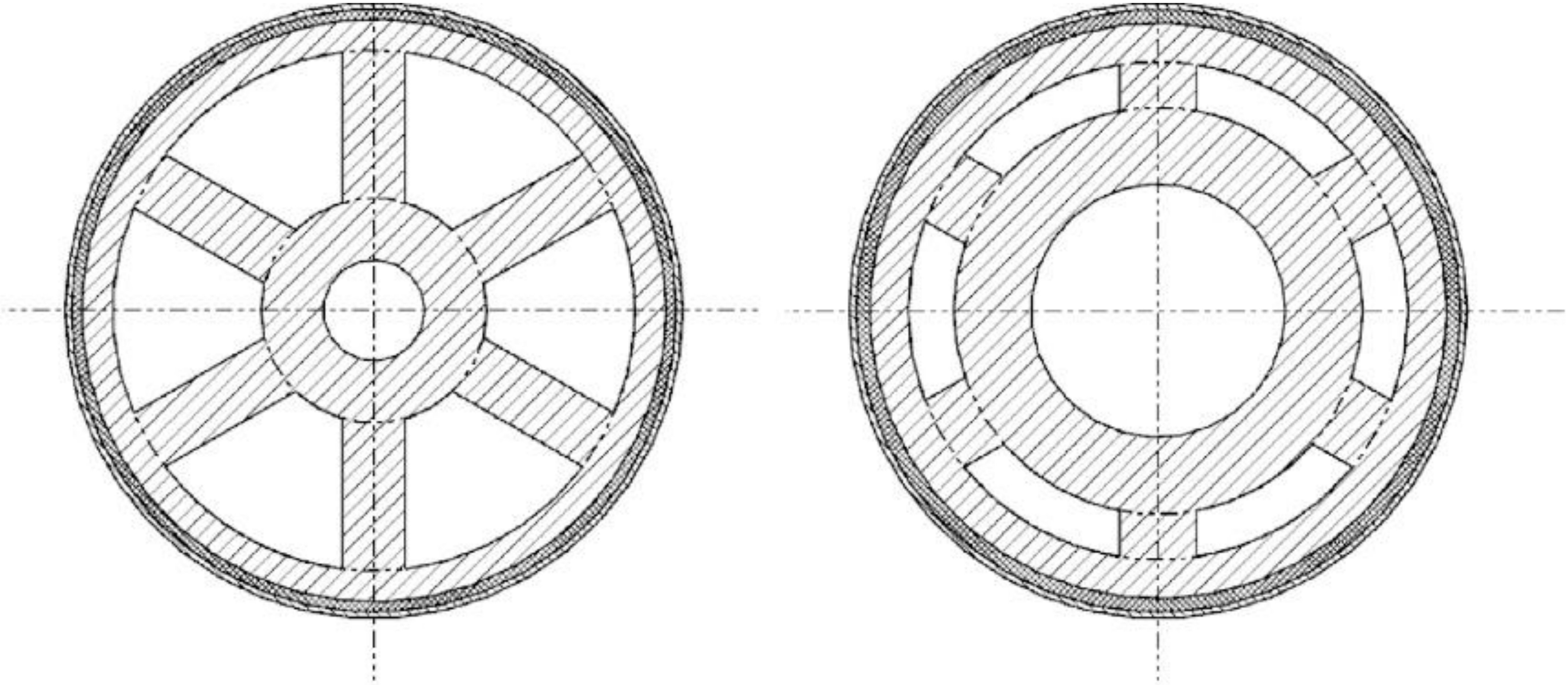

Fig. 9. Comparison of hybrid rocket motor grains enabling equal fuel volumetric fractions of the combustion chamber, despite different burn durations: a) main core without boosters b) main core with SRM boosters.

From: Okninski, Acta Astronautica, 145 (2018) 1-10

There are severe problems of peel off of the not-truly strong (nearly brittle desirably) of thin layers during final burn period. Sliver losses will be high. Avoiding this calls for a proper design of perhaps a star shaped grain

Tian H, Li X T, Yu N J, et al. Numerical and experimental investigation on the effects of aft mixing chamber diaphragm in hybrid rocket motor. Sci China Tech Sci, 2013, 56: 2721–2731, doi: 10.1007/s11431-013-5325-z

My comment: An excellent piece of R & D

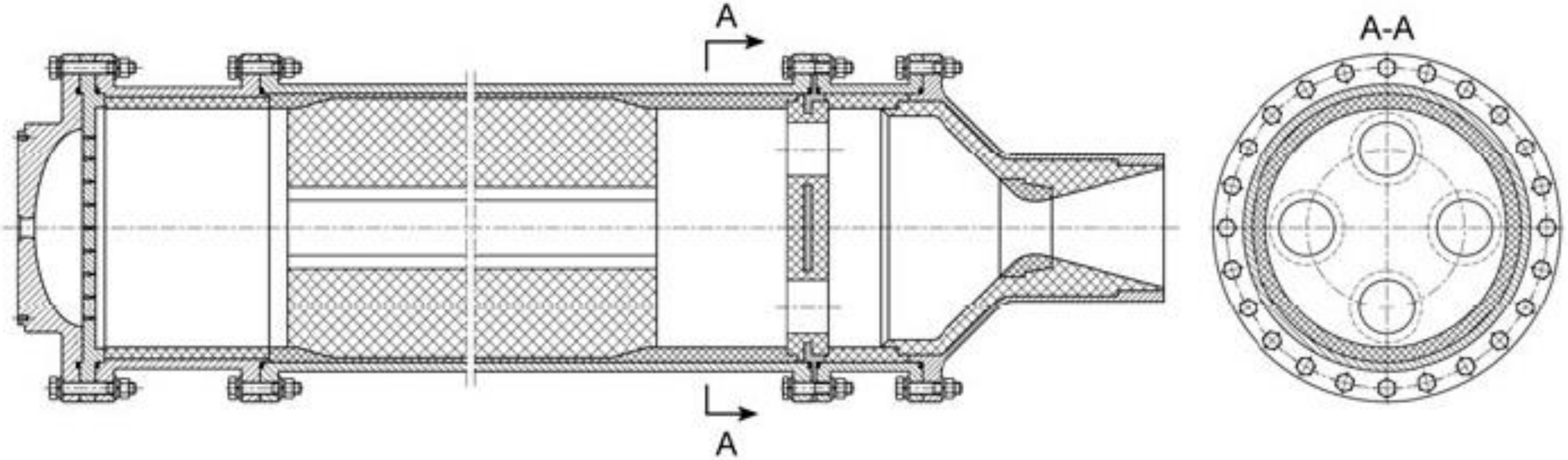

H_2O_2 – HTPB propellants
Star grain without and with diaphragm

For computation they use

$\dot{m}_{ox} = 2$ kg/s,

$Y_{ox} = 0.42$, $H_2O = 0.58$,
$T = 1000$ K

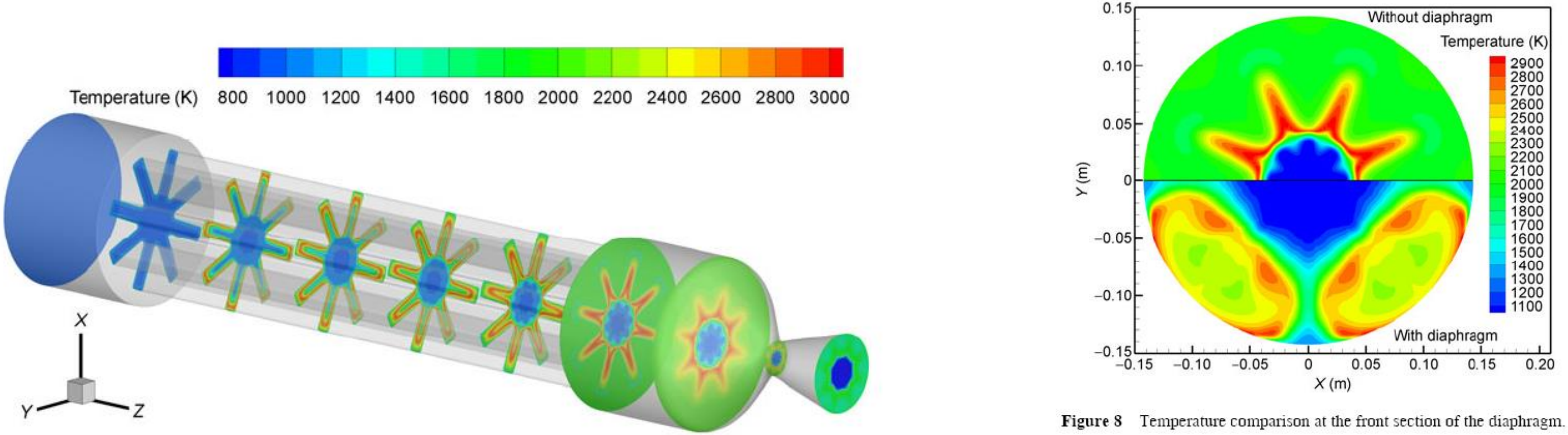

Figure 8 Temperature comparison at the front section of the diaphragm.

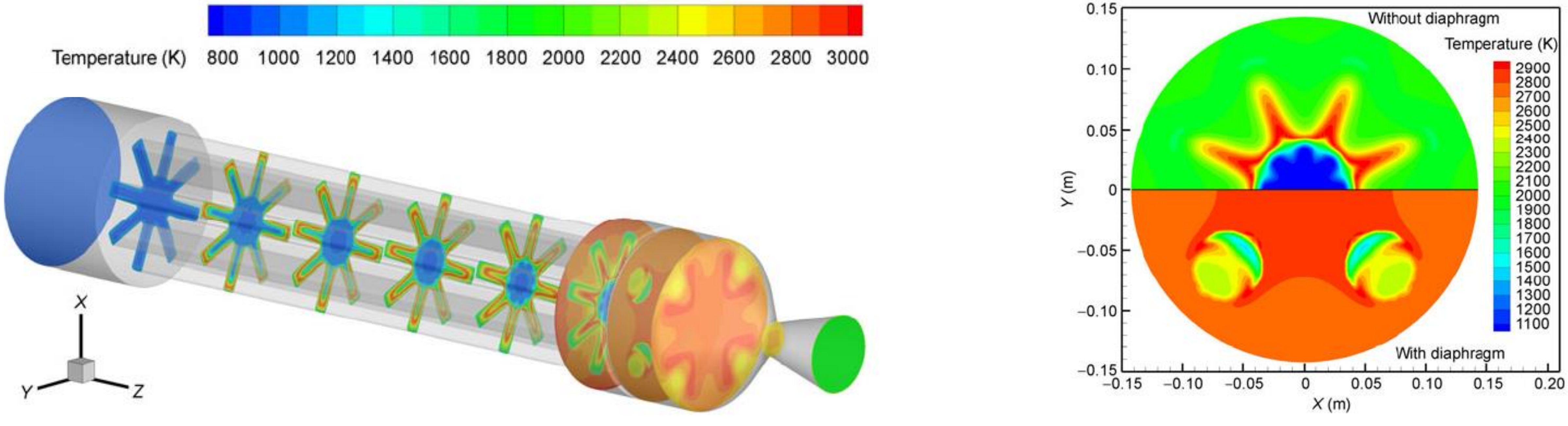

Figure 9 Temperature comparison at the back section of the diaphragm.

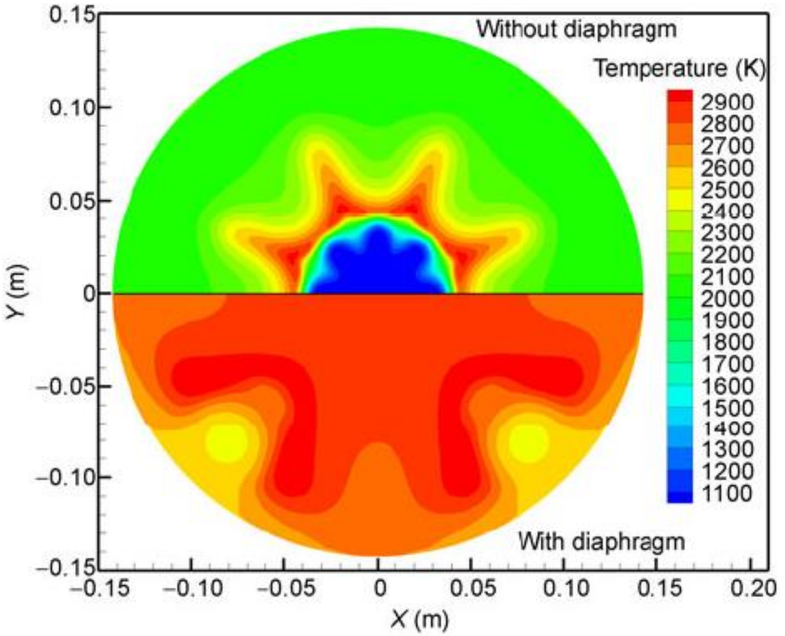

Figure 10 Temperature comparison of the nozzle entrance.

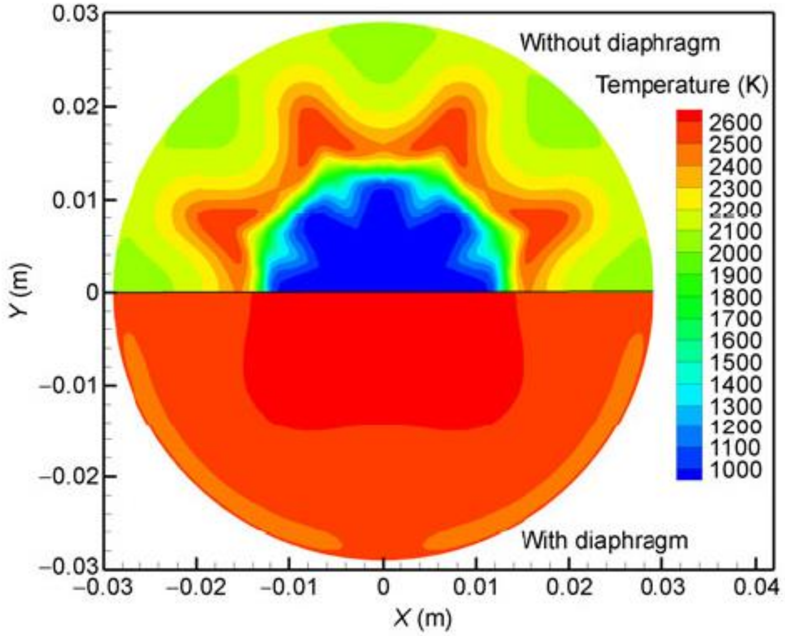

Figure 11 Temperature comparison of the nozzle throat.

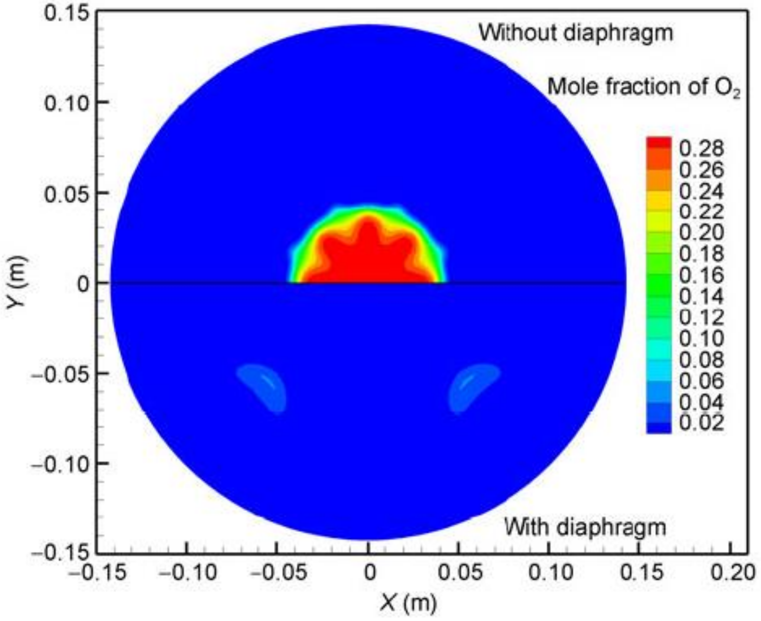

Figure 17 Mole fraction comparison of O_2 in the nozzle entrance.

Table 2 Motor performances of the simulation results

Parameters	Without diaphragm	With diaphragm
$\dot{m}_o$ [kg s^{-1}]	2.0	2.0
OF	4.58	4.58
c^* [m s^{-1}]	1296.1	1535.1
I_s [m s^{-1}]	2051.1	2417.7
η_{c^*} [%]	82.62	97.84
η_{I_s} [%]	79.67	93.90

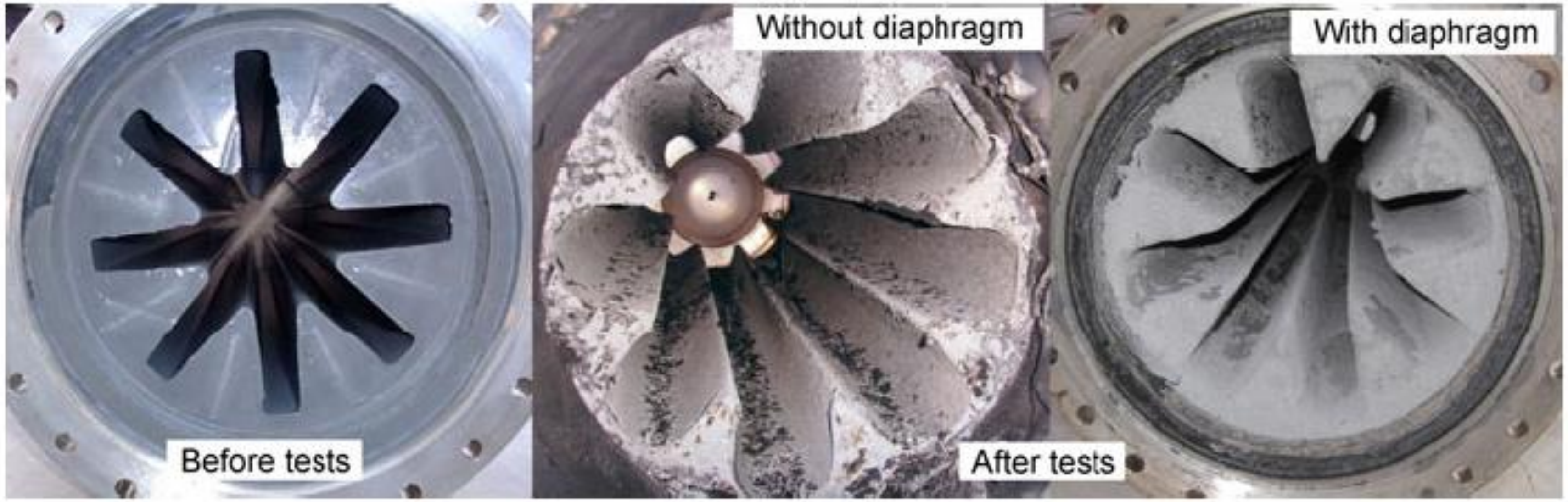

Figure 22 Fuel grains before and after tests.

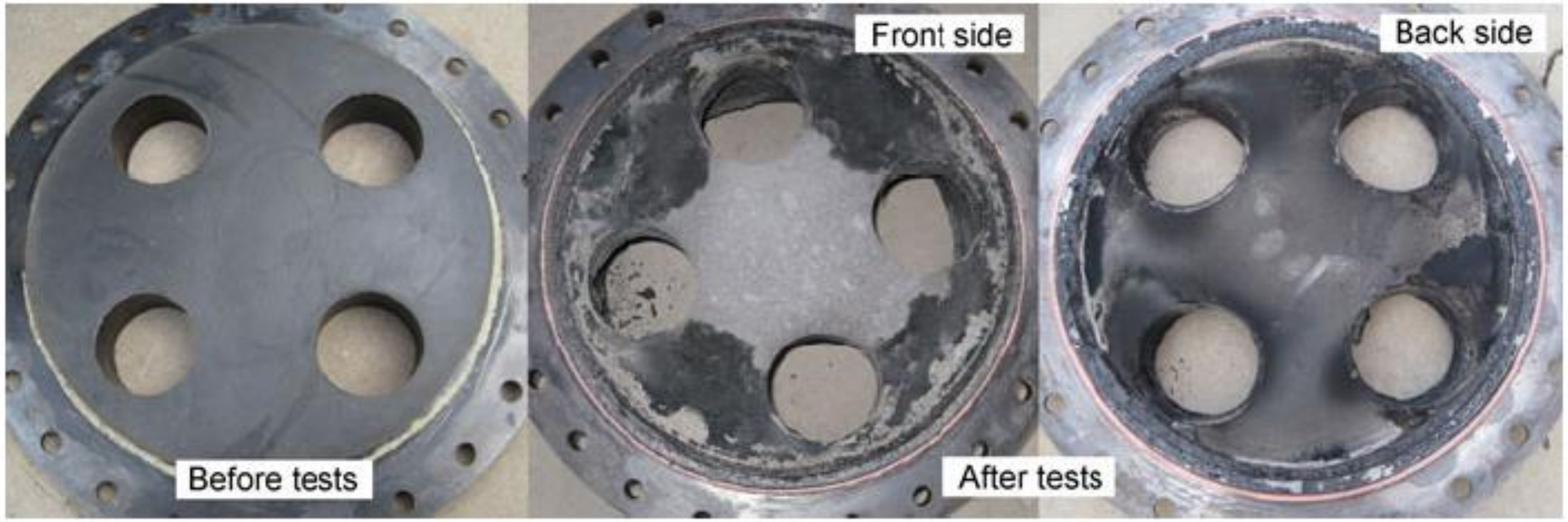

Figure 23 Diaphragm before and after tests.

Experimental details
different from simulation

Fuel used: 60 HTPB, 28 Al, 10 Mg, 2C

Diaphragm: Steel framework
+ EPDM rubber over it.

Burn time with diaphragm: 10 s
Burn time without diaphragm = 30 s

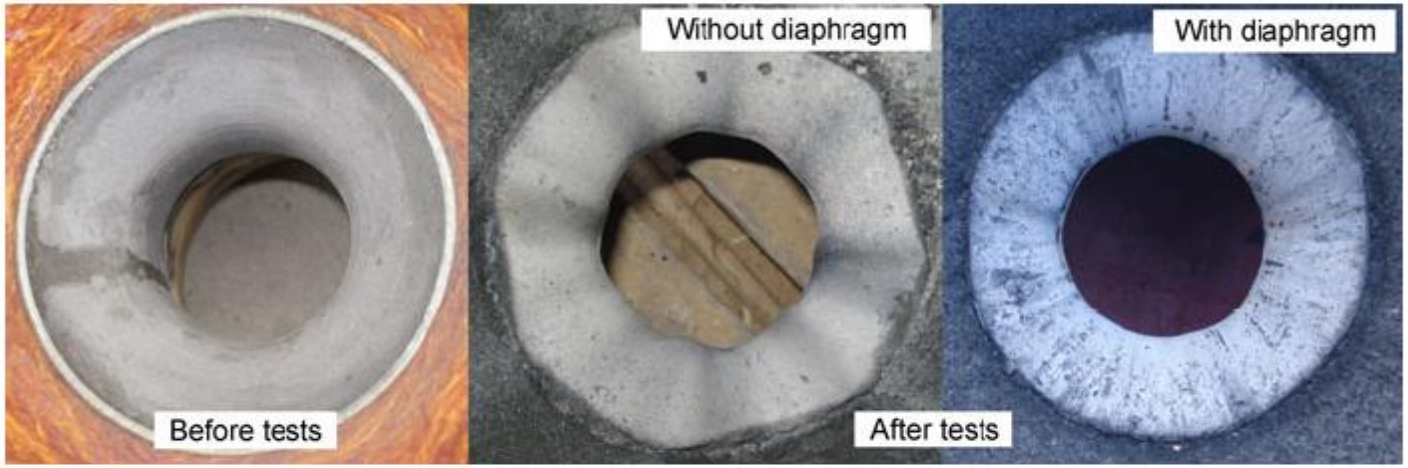

Figure 24 Nozzle throats before and after tests.

Table 3 Motor performances of the experimental results

Parameters	Without diaphragm	With diaphragm
m_o[kg s^{-1}]	1.997	2.025
OF	3.148	2.290
t [s]	30	10
p_c [MPa]	1.401	1.690
F [N]	4.753	5.602
c^* [m s^{-1}]	1518.3	1555.4
I_s [m s^{-1}]	1779.9	1932.5
η_{c^*}[%]	93.90	97.34
η_{I_s}[%]	80.77	87.28

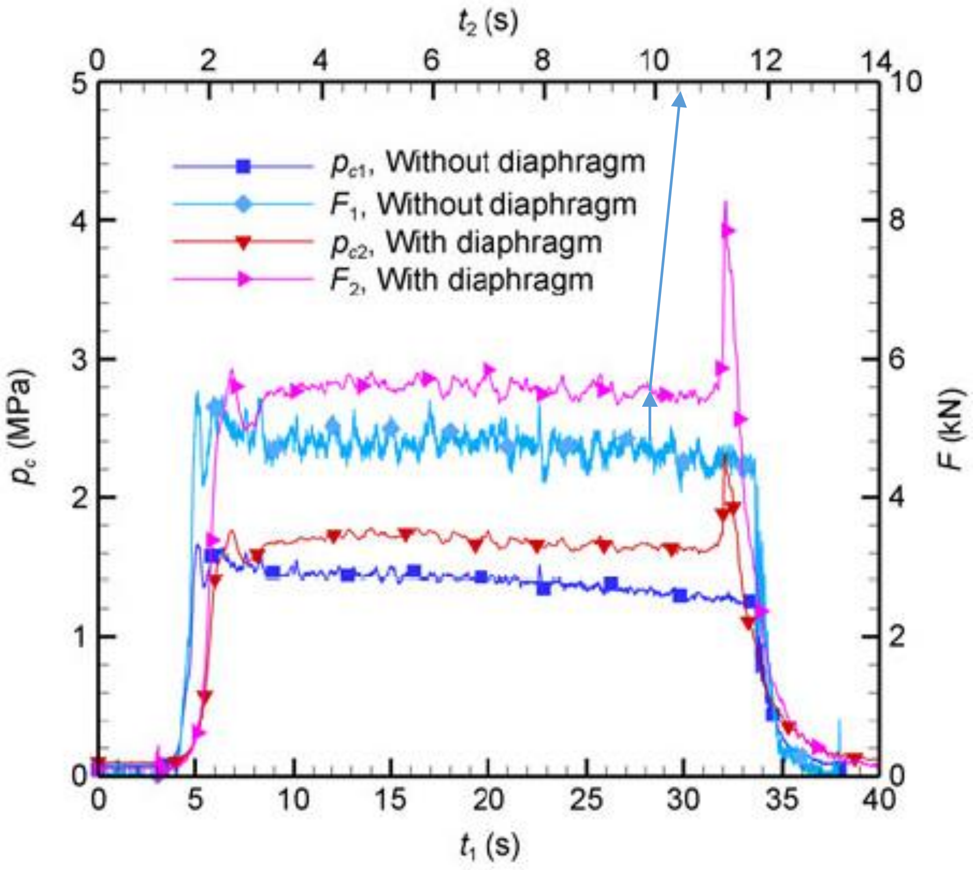

Figure 25 Experimental curves of the two motors.

Table 2 Motor performances of the simulation results

Parameters	Without diaphragm	With diaphragm
$\dot{m}_o$[kg s^{-1}]	2.0	2.0
OF	4.58	4.58
c^* [m s^{-1}]	1296.1	1535.1
I_s [m s^{-1}]	2051.1	2417.7
η_{c^*} [%]	82.62	97.84
η_{I_s} [%]	79.67	93.90

3-d numerical simulation of 2-phase flow in hybrid rocket motor

Xintian Li[1], Hui Tian[2], Nanjia Yu[3], Guobiao Cai[4]
School of Astronautics, Beihang University, Beijing, 100191, China

AIAA 2013-3893

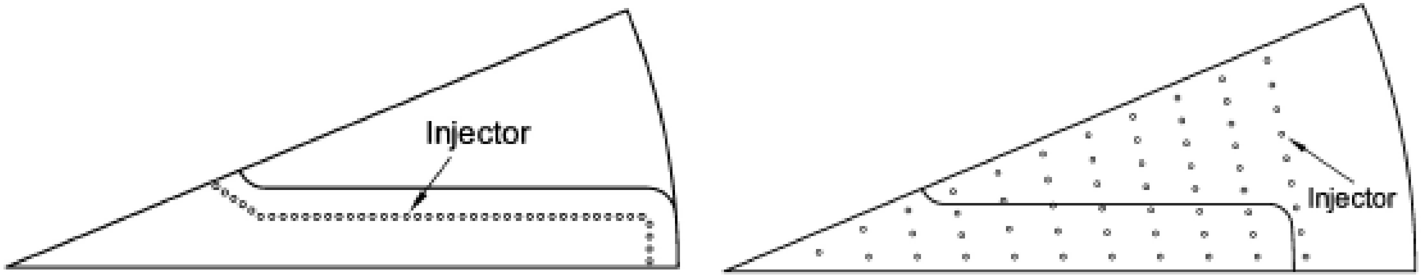

a), Injector pattern A b), Injector pattern B

Figure 3 Two kinds of injector patterns

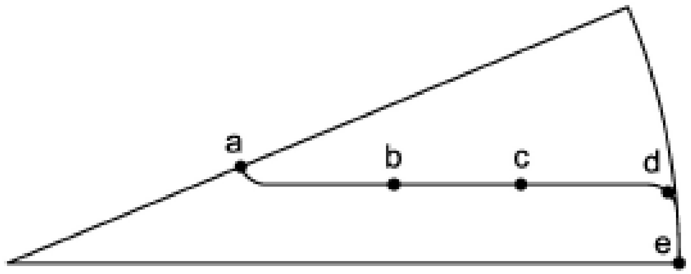

Figure 4 Definition of the points on the solid fuel surface

with hydrogen peroxide (H_2O_2) as the liquid oxidizer and hydroxyl terminated polybutadiene (HTPB) as the solid fuel. Two kinds of injector patterns are designed for the

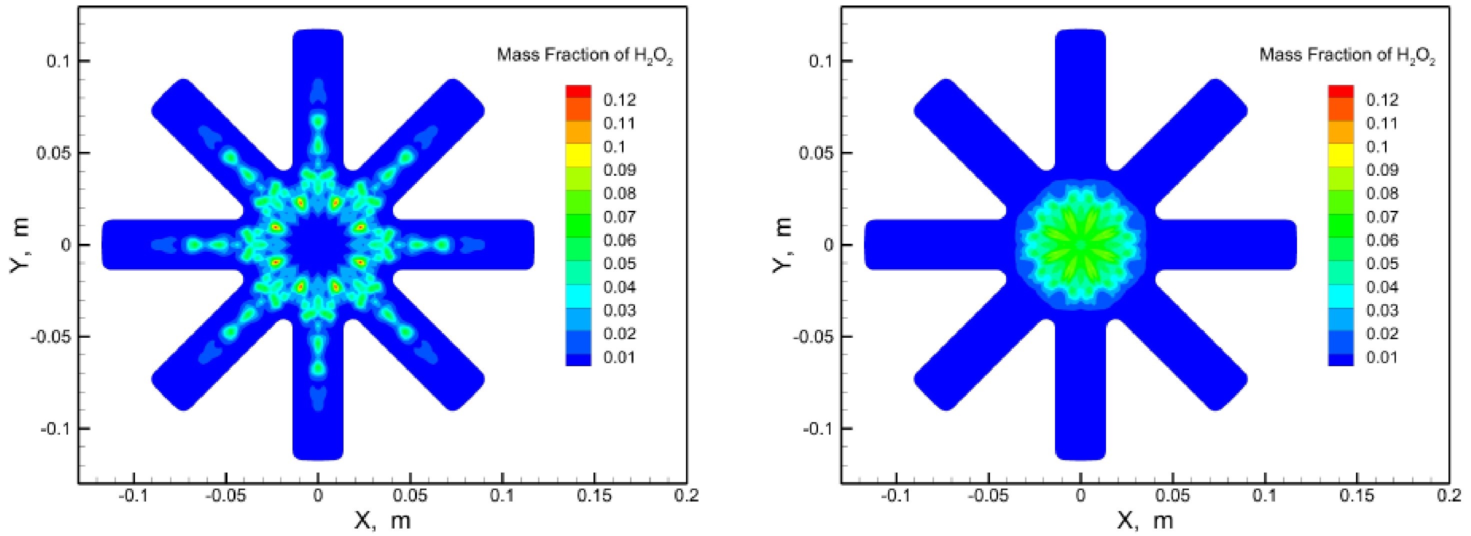

a) Injector pattern A b) Injector pattern B

Figure 7 Mass fraction of H_2O_2 in the central cross section of the fuel port (Z=0.7m)

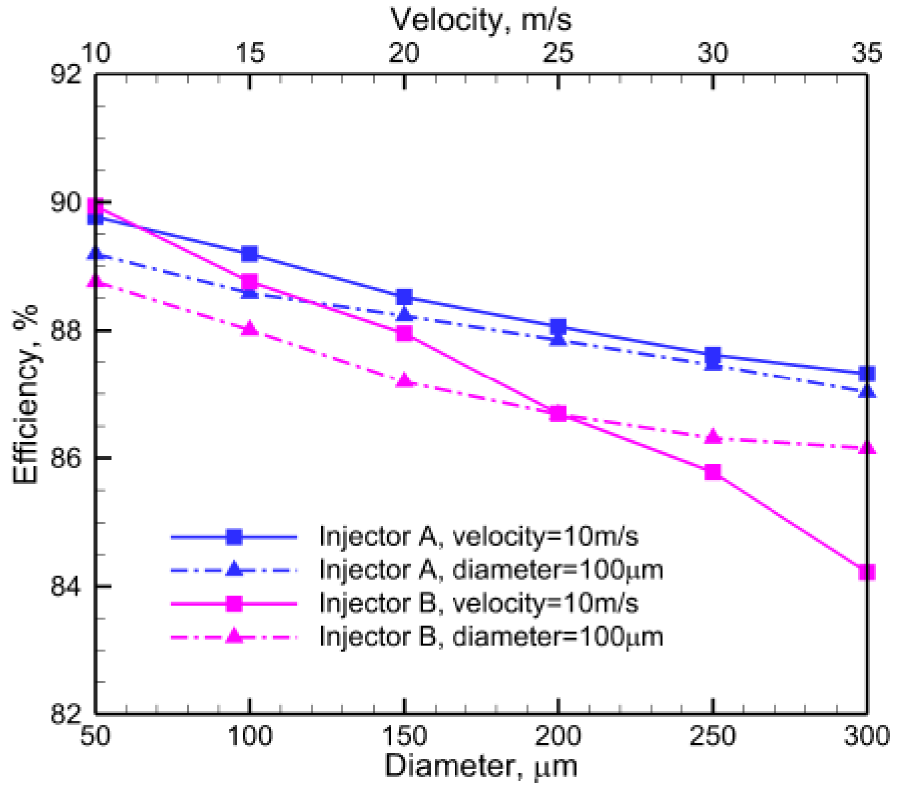

Figure 12 Combustion efficiencies of different njection parameters

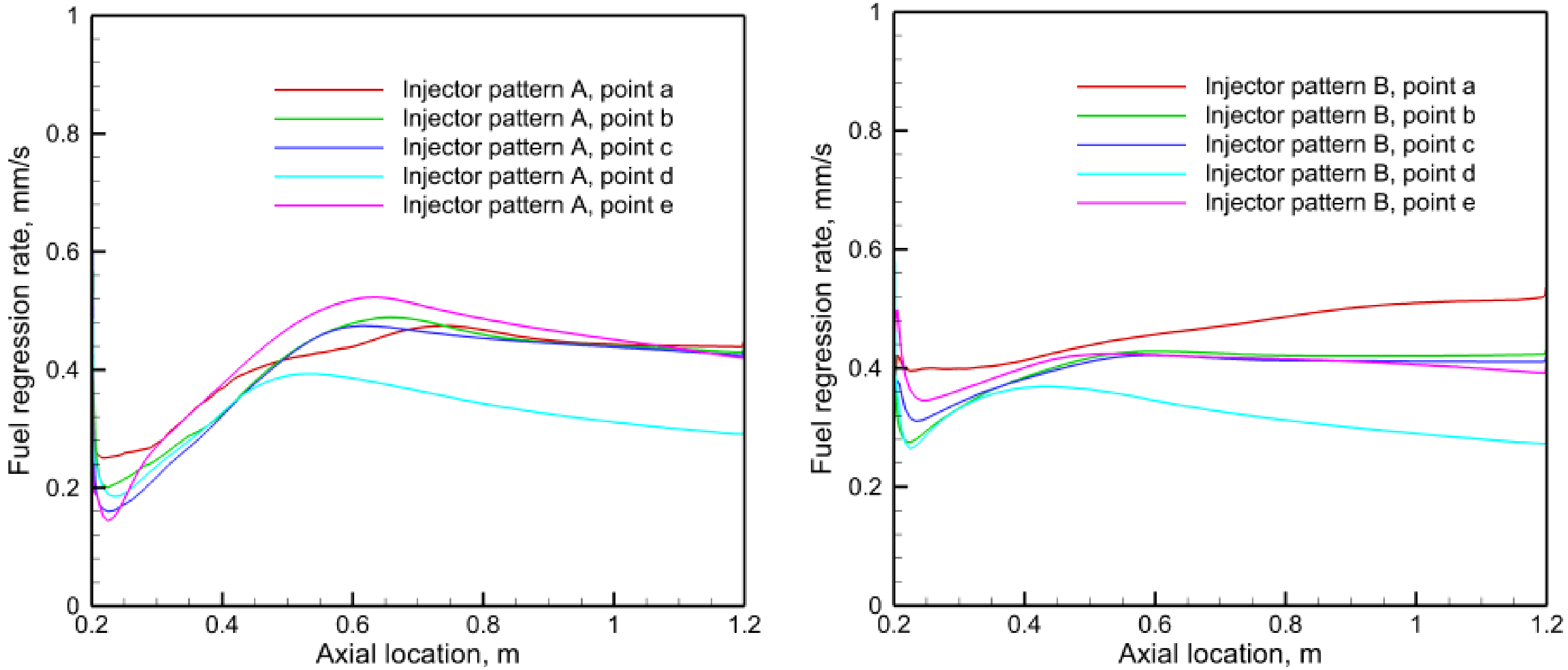

a) Injector pattern A b) Injector pattern B

Figure 9 Fuel regression rates of different points along axial location

Conclusion:
Injector A is better

Such studies will add value

Summary

- The burn rates of fuels with oxygen/N_2O can vary widely from 0.3 mm/s to 3 mm/s at 100 kg/m^2s of oxidizer flux.
- An index of n = 0.5 in $\dot{r} = aG_{ox}^{n}$ would be most appropriate for reasonably large fluxes. Index increases to 0.7 at low fluxes (< 50 kg/m^2s).
- Measuring the regression rates at smaller sizes may not add much value. Performing these at right scale of use would be the most appropriate strategy. CFD as an auxiliary tool would add value.
- All issues like web stability during tail-off and performance will become simultaneously revealed.
- Such a strategy is time and resource optimal too.

References

1. 1967: G. A. Marxman, 10th symp. Combustion, boundary layer combustion in propulsion
2. 1982: P. J. Paul et al, 19th symp. Comb, regression rates in boundary layer combustion.
3. 2010: B. Cantwell, A. Karabeyoglu, and David Altman, Int. J. Energetic materials 305-326 Recent advances in hybrid propulsion
4. 2011: Max Calabro, Overview on hybrid propulsion, Prog. In Propulsion physics, 2, 353-374
5. 2012: L. Fanton, C. Paravan, and L. D. Luca, Int J. Aerospace Engg, Testing and modeling…
6. 2012: D. Pastrone, Int. J. Aerospace Engg, Approaches to low fuel reg. rate in hybrid….
7. 2013: Scaramuzzino, et al, AIAA 2013-4039, Fuel reg … on lab hybrid with N2O and Wax..
8. 2013: Tian et al, Numerical and experimental …aft mixing chamber, Sci China Tech Sci, 2721
9. 2013: Li, Tian et al, 3-d numerical simulation of 2-phase flow ..motor, AIAA 2013-3893

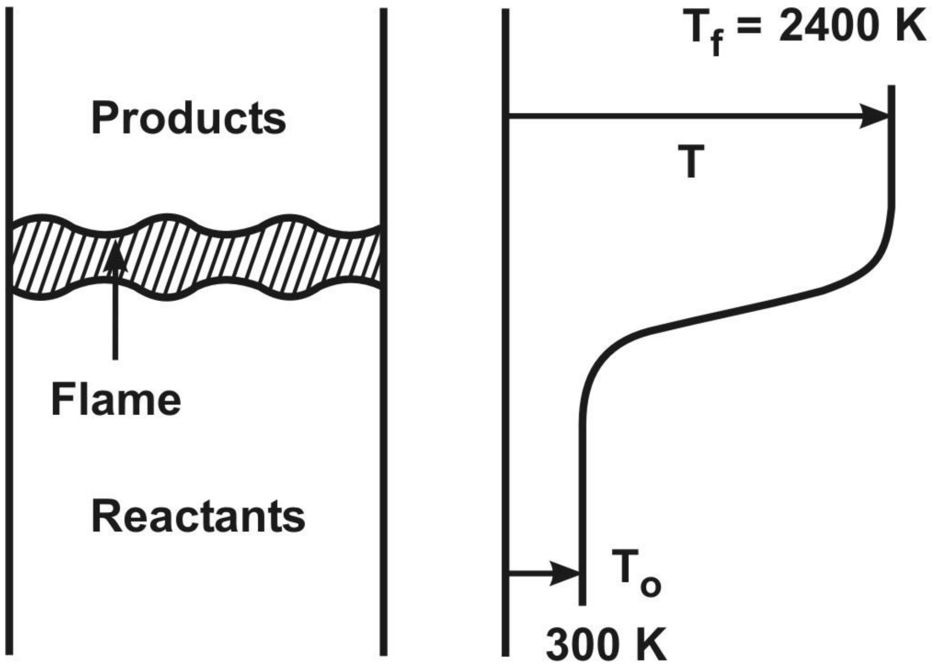

(a) Gaseous flame

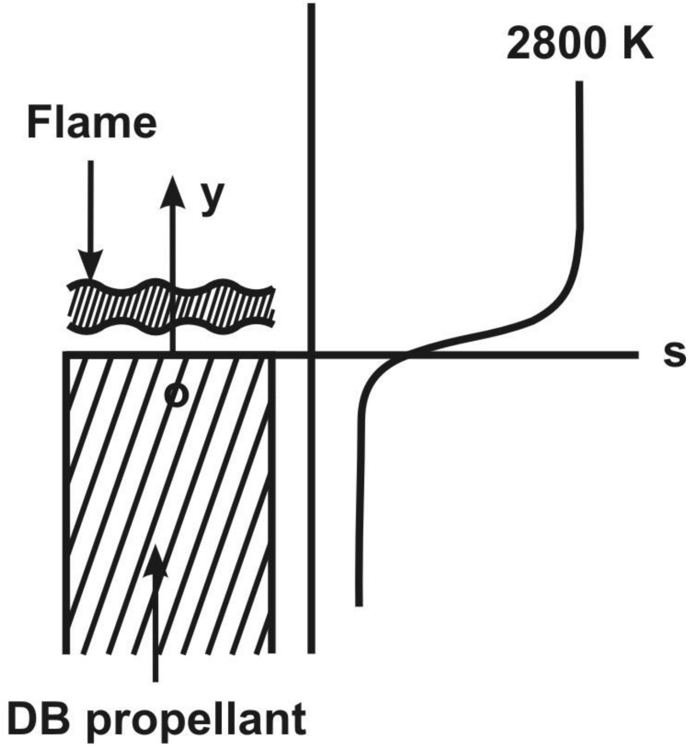

(b) Solid propellant

Simple analysis of the **premixed** and diffusion limits

The heat flux at the surface can be written as

$$\rho_p \dot{r}(-H_s) = \dot{q}''_g - \dot{q}''_s = k\frac{dT}{dx}\Big]_{0+} - k\frac{dT}{dx}\Big]_{0-} \tag{1}$$

where $\dot{q}''_g$ and $\dot{q}''_g$ are the gas phase and condensed phase heat fluxes with the left hand side being the heat flux due to decompositional phase change at the surface. The solution for the gas phase equation involving conduction - convection balance follows the procedure used in BDP model (Beckstead et al, . . .)

$$\frac{T - T_s}{T_f - T_s} = \frac{e^{\xi} - 1}{e^{\xi*} - 1}; \quad \xi = \frac{\rho_p \dot{r} c_p x}{k} \tag{2}$$

The heat flux from the gas phase is given by

$$k\frac{dT}{dx}\Big]_{0+} = \frac{(T_f - T_s)}{e^{\xi*} - 1} \tag{3}$$

The flame stand-off distance, $x = x^*$ is expressed by

$$x^* = \rho_p \dot{r}/(K_r p^{n_r}); \quad K_r = A_r e^{-E_g/(RT_f)} \tag{4}$$

Therefore we get ξ^* as

$$\xi^* = (\rho_p \dot{r})^2 c_p/(k K_r p_r^n) \tag{5}$$

It can be noted that K_r, the gas phase reaction constant K_r is dependent on gas phase activation energy E_g. The pyrolysis law for the surface regression rate is

$$\dot{r} = A_s e^{-E_s/(RT_s)} \tag{6}$$

$$\rho_p \dot{r}(-H_s) = \rho_p \dot{r} \frac{c_p(T_f - T_s)}{e^{\xi^*} - 1} - \rho_p \bar{\dot{r}} c_p(\bar{T}_s - T_0)$$

which on simplification gives

$$e^{\xi^*} - 1 = \frac{c_p(\bar{T}_f - \bar{T}_s)}{[c_p(\bar{T}_s - T_0) - H_s]} g_f \bar{f}_{nll} = B_f; \;\; \xi^* = ln(1 + B_f) \tag{16}$$

Hence we get

$$[\rho_p \bar{\dot{r}}]^2 = (k/c_p) ln(1 + B_f) \bar{K}_r \bar{p}^{n_r} \tag{17}$$

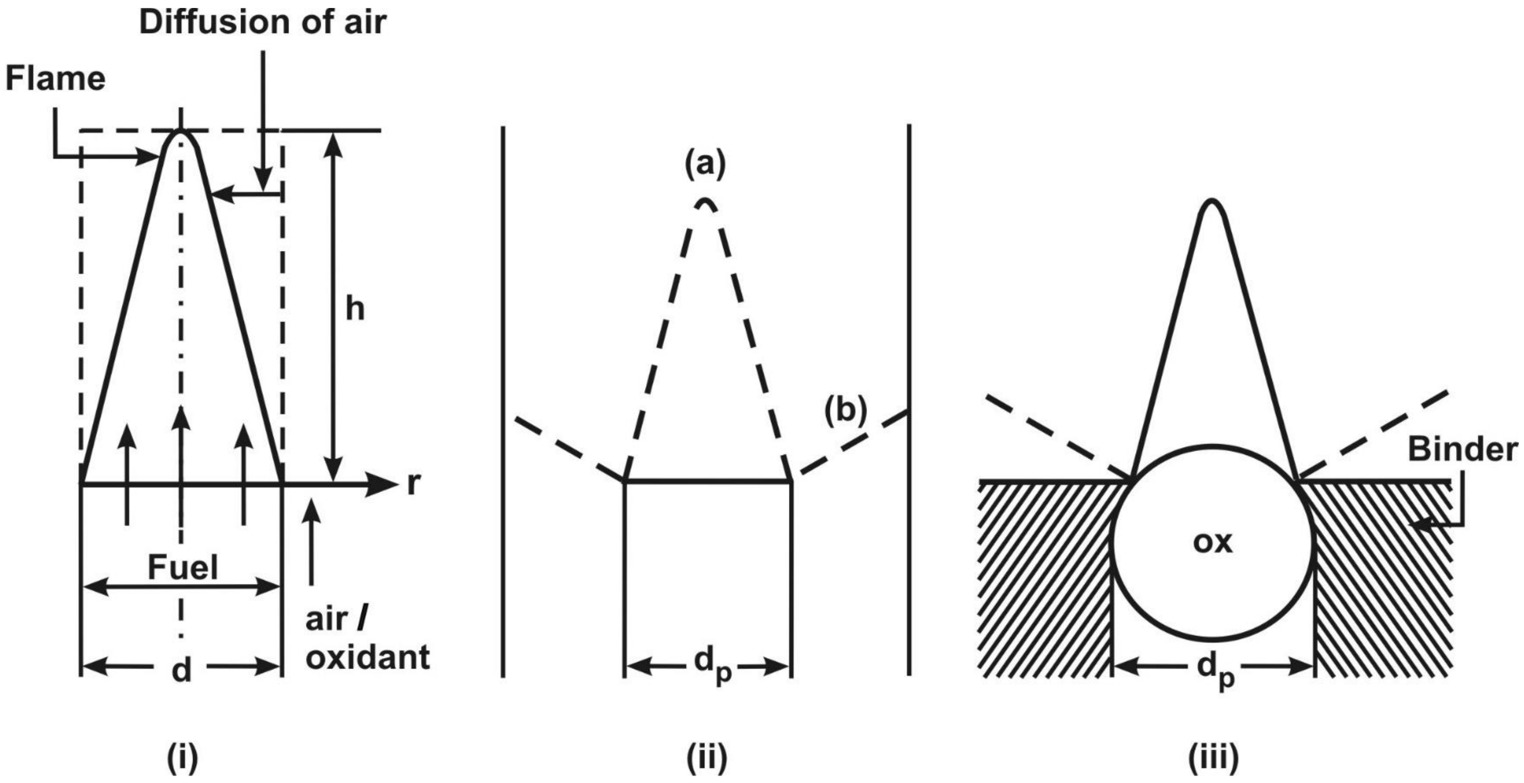
Diffusion of air
Flame
h
r
Fuel
air /
oxidant
d
(i)
(a)
(b)
d_p
(ii)
Binder
ox
d_p
(iii)

Simple analysis of the premixed and **diffusion limits**

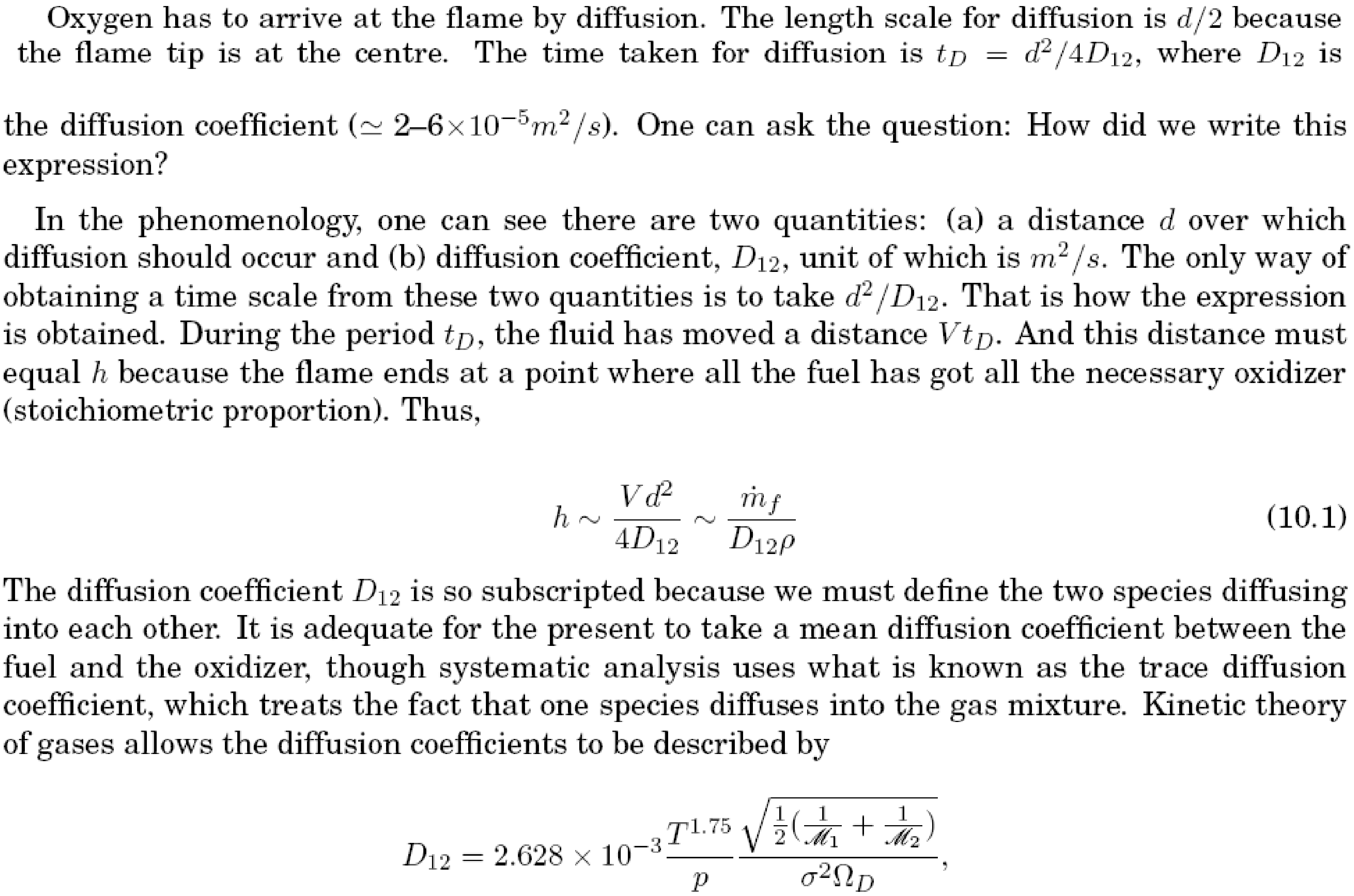

Oxygen has to arrive at the flame by diffusion. The length scale for diffusion is $d/2$ because the flame tip is at the centre. The time taken for diffusion is $t_D = d^2/4D_{12}$, where D_{12} is the diffusion coefficient ($\simeq$ 2–6$\times 10^{-5} m^2/s$). One can ask the question: How did we write this expression?

In the phenomenology, one can see there are two quantities: (a) a distance d over which diffusion should occur and (b) diffusion coefficient, D_{12}, unit of which is m^2/s. The only way of obtaining a time scale from these two quantities is to take d^2/D_{12}. That is how the expression is obtained. During the period t_D, the fluid has moved a distance Vt_D. And this distance must equal h because the flame ends at a point where all the fuel has got all the necessary oxidizer (stoichiometric proportion). Thus,

$$h \sim \frac{Vd^2}{4D_{12}} \sim \frac{\dot{m}_f}{D_{12}\rho} \tag{10.1}$$

The diffusion coefficient D_{12} is so subscripted because we must define the two species diffusing into each other. It is adequate for the present to take a mean diffusion coefficient between the fuel and the oxidizer, though systematic analysis uses what is known as the trace diffusion coefficient, which treats the fact that one species diffuses into the gas mixture. Kinetic theory of gases allows the diffusion coefficients to be described by

$$D_{12} = 2.628 \times 10^{-3} \frac{T^{1.75}}{p} \frac{\sqrt{\frac{1}{2}(\frac{1}{\mathscr{M}_1} + \frac{1}{\mathscr{M}_2})}}{\sigma^2 \Omega_D},$$

$$\frac{h}{d} = \frac{ReSc}{4} \tag{10.2}$$

where $Sc = \mu/D_{12}\rho = \nu/D_{12}$ = Schmidt number is a term of the order unity ($\sim$ 0.75–1.2). One would see that the expression shows no dependence on fuel properties. This is simply because we have not accounted for it yet. For the same flow rate and diameter of the duct, if requirements of stoichiometry are higher (implying more air is required to burn a fixed amount of fuel), then the flame height has to be larger. Also, if the active oxidizer mass fraction in the surrounding air, $Y_{0\infty}$, is increased, one would expect the flame height to be lower. Thus one would expect

$$h = \frac{ReSc}{4 f_s Y_{0,\infty}^{m_2}}$$

We will present a simple argument which includes these effects and obtain the expression for flame height.

Suppose the flame is enclosed in a cylinder of diameter d and height h. The fuel flow rate is $\dot{m}_f$. The flame will acquire just enough air for it to burn completely. This means that the air obtained by diffusion should be in stoichiometric proportion with fuel flow. This means

$\dot{m}_{air}/\dot{m}_f = 1/f_s$. The flow rate of air is the product of mass flux, and the area, πhd. The mass flux is given by Fick's law of diffusion as $D_{12}\rho(dY_0/dx)$. We can take take $dY_0 = (Y_{0,\infty} - 0)$, $dx = d/2$ and write down the relationship for the stoichiometric air-to-fuel flow rate as

$$\pi hd \times 2D_{12}\rho \times \frac{Y_{0\infty}}{d} = \dot{m}_{air} = \frac{\dot{m}_f}{f_s} \tag{10.3}$$

Thus,

$$h = \frac{\dot{m}_f}{2\pi f_s Y_{0\infty} D_{12}\rho}, \qquad \frac{h}{d} = \frac{ReSc}{8 f_s Y_{0\infty}} \tag{10.4}$$

$$k\left[\frac{dT}{dy}\right]_{y=0} = \dot{q}'' = \rho_p \dot{r} L$$

where $\rho_p \dot{r}$ is the product of the density of solid and solid regression rate and L, the heat of phase change from solid to gas and $\dot{q}''$, the heat flux expressed in terms of Fourier's law of conduction. Noting that dy can be replaced by a quantity proportional to h and dT replaced by the difference between an effective flame temperature and surface temperature, one can write $k(T_f - T_s)/h = \rho_p \dot{r} L$. So one gets

$$\rho_p \dot{r} = k(T_f - T_s)/hL$$

Noting that $\dot{m}_f = \rho_p \dot{r}(\pi/4)d^2$ where d the particle size, we can express the earlier equation for h as

$$h = \frac{\rho_p \dot{r} d^2}{8 f_s Y_{0,\infty} D_{12} \rho} \tag{10.5}$$

If we use this expression in the expression for burn rate we get

$$\rho_p \dot{r} = \frac{1}{d}\sqrt{8(k/c_p) f_s Y_{0,\infty} D_{12} \rho} \tag{10.6}$$

Since h is independent of pressure, it follows that $\rho_p \dot{r}$, the mass burning rate (or mass flux) as it is called, is independent of pressure as is evident from the above equation. An additional result that can be obtained from this equation is taht the burn rate increases with decrease in particle size. This result is applicable till a point when premixedness takes over (that happens below a particle size).